

Chapter 4

Anisotropically Ion-Conductive Polymer Films

Abstract: Polymerizable smectic and columnar liquid crystals with an imidazolium ionic moiety were designed to obtain two- and one-dimensionally ion-conductive polymer films. The smectic monomers spontaneously formed homeotropic monodomains on a glass substrate in the smectic A phases. As for the columnar monomer, a homogeneous monodomain on the substrate was obtained by shearing the material in the columnar phase. Mechanically stable polymer films were prepared by photopolymerization of the aligned monomers in the liquid crystalline states. Scanning electron microscopic observation revealed that macroscopically aligned nanostructures were formed in these films. Ionic conductivities were measured for the monomers and polymer films as a function of temperatures. These materials showed high ionic conductivities along the direction parallel to the smectic layer and columnar axis.

4.1. Introduction

Ion-conductive polymers such as poly(ethylene oxide)s (PEOs) have advantages for applications as solid electrolytes in batteries^{1,2} and electrochromic devices³ because of their processibility and lightness. For further functionalization of ion-conductive polymers, the introduction of ordered nanostructures that provide anisotropic conductivities in low dimensions is of interest. Self-organization processes of liquid crystals can be used to obtain such anisotropic materials.⁴⁻¹⁸ Recently, Kato and coworkers have reported the first example of an anisotropic ion-conductive film, which has layered nanostructures.⁵ This film was obtained by in situ photopolymerization of oriented liquid crystalline smectic complexes, which consist of a PEO-based liquid crystalline monomer and lithium triflate.

On the other hand, ionic liquids are ion-conductive organic liquids composed of ions. They have attracted much attention as new liquid electrolytes due to their unusual characters such as non-volatility, non-flammability, and high ionic conductivity.¹⁹⁻²⁵ The author prepared high ion-conductive liquid crystalline materials through self-assembly of isotropic ionic liquids and hydroxyl-terminated liquid crystals (chapter 2) or ionic liquid crystals (chapter 3).

Polymer electrolytes based on ionic liquids have been prepared as a new family of ion-conductive polymers.²²⁻²⁴ The author intends to obtain two- and one-dimensionally ion-conductive polymer films based on ionic liquids. The design is to incorporate ionic moieties used to form ionic liquids into side-chain liquid crystalline polymers and tapered dendritic polymers. There are a few reports on side-chain ionic liquid crystalline polymers.²⁶⁻²⁹ These materials may have potentials for application as solid polymer electrolytes. However, no anisotropic ion conduction was achieved for these polymers.

4.2. Results and Discussion

4.2.1. Two-Dimensionally Ion-Conductive Polymer Films

In the present study, polymerizable liquid crystalline monomers **1–3** with an imidazolium tetrafluoroborate moiety at the extremity of the alkyl or oligo(ethylene oxide) chains (Figure 4–1) have been prepared to form two-dimensionally ion-conductive polymers **poly1–3**. Imidazolium salts containing weakly coordinating perfluorinated anions are promising candidates to form ionic liquids showing high ionic conductivities. The author expected that the introduction of the salt moiety into mesogenic rodlike molecules led to the formation of ion-active layered nanostructures. It is also expected that the use of oligo(ethylene oxide) chain as a flexible spacer between the ionic moiety and the mesogenic core may enhance the ionic conductivity due to the increase of mobility of the ionic moiety.

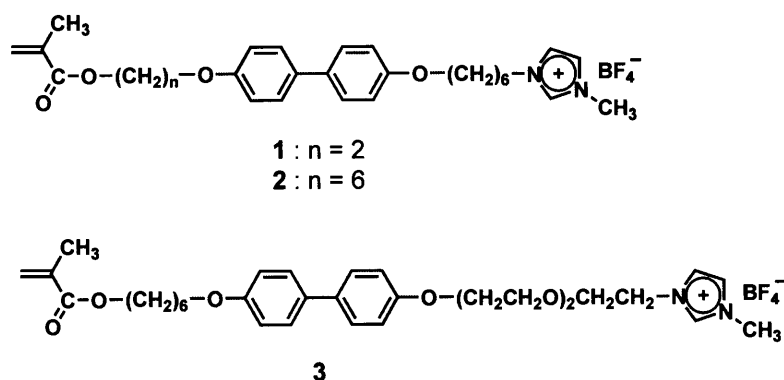


Figure 4–1. Molecular structures of liquid crystalline monomers with an imidazolium tetrafluoroborate moiety.

Liquid Crystalline Properties

Phase transition temperatures of the synthesized compounds are summarized in Table 4–1. Compound **1** exhibits a monotropic smectic A phase (S_A) from 60 to 52 °C. On subsequent cooling, **1** shows two unidentified smectic phases (S_X) from 52 to 39 °C and a crystalline phase (Cr) below 39 °C. On the other hand, compounds **2** and **3** show enantiotropic

smectic phases. For compound **2**, two smectic A phases (S_{A1} and S_{A2}) were observed. X-ray diffraction patterns of these phases showed that in the S_{A1} phase, an interdigitated bilayer structure with a layer spacing of 3.6 nm is formed and a bilayer structure with a layer spacing of 5.5 nm is formed in the S_{A2} phase.

Figure 4–2 shows the optical textures of **1** in the S_A phase at 58 °C under crossed polarizers, which reveal the difference of the molecular orientation on glass and indium tin oxide (ITO) surfaces. The dark region shown in Figure 4–2(a) indicates that **1** spontaneously forms a homeotropic alignment on a glass surface. This alignment was confirmed by the conoscopic observation on a polarizing microscopy. On the other hand, as shown in Figure 4–2(b), the fan-shaped texture indicating the formation of unaligned polydomains is observed on the ITO surface. Such homeotropic alignment can be attributed to hydrophilic nature of the glass surface, which is capable of interacting with the ionic moiety at the extremity of molecule. Also compounds **2** and **3** spontaneously form homeotropic alignment on the surface of a glass substrate and no vertical alignment is achieved on the surface of the ITO substrate.

Table 4–1. Phase transition behavior of compounds **1**, **2**, and **3**.

Compound		Phase transition temperature /°C ^a							
1a (n = 2)	I	60	S_A^b	52	S_{X1}^b	49	S_{X2}^b	39	Cr
1b (n = 6)	I	108	S_{A2}	96	S_{A1}			82	Cr
2	I	79	S_A					51	Cr

^aPhase transition temperatures were determined by DSC measurement on cooling at a scanning rate of 10 °C min⁻¹. ^bMonotropic liquid crystalline phases. S_A , S_{A1} , S_{A2} : smectic A phases; S_{X1} , S_{X2} : unidentified smectic phases; Cr: crystalline phase; I: isotropic liquid phase.

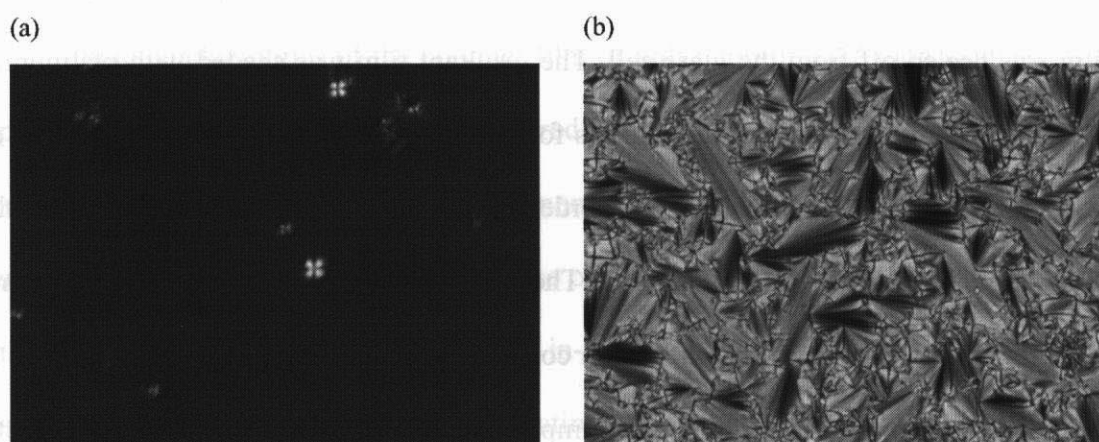


Figure 4–2. Optical textures of monomer **1** in the S_A phase at 58 °C under crossed polarizers: (a) homeotropically aligned monodomain on a glass substrate; (b) unaligned polydomains on an ITO electrode.

Fixation of Layered Structures by Photopolymerization

No macroscopic uniform orientation of anisotropic nanostructures was observed for ion-conductive liquid crystalline polymers prepared by solution polymerization.^{9,10,29} In these cases, the ionic conductivities were lower than expected, and no anisotropic conductivity was observed. The boundaries present in the random polydomains disturbed ion conduction. In contrast, to obtain liquid crystalline polymers with macroscopically oriented nanostructures, in situ photopolymerization of oriented liquid crystalline monomers was employed.^{30–33} This method was successfully used to obtain anisotropic ion-conductive polymer films with well-defined layered nanostructures.⁵

A photoinitiator, 2,2-dimethoxy-2-phenylacetophenone was added to monomers (0.5 wt %). The mixture was placed both in the glass and ITO cells. In situ photopolymerization of the mixtures containing **1** or **2** in the S_A phases and the mixture containing **3** in the S_{A2} phase was carried out by UV light irradiation (around 365 nm, 35 mW/cm²) with a super high-pressure mercury lamp for 15 minutes. Mechanically stable elastic polymer films were obtained after photopolymerization of all monomers.

SEM measurement was performed for the polymer film of **poly1**. The free-standing film was peeled off from the glass cell. The resultant film was shaded with platinum. Figure 4-3 shows that a layered nanostructure is formed in the photopolymerized film. The average distance between two lines is in the order of 50 nm. The layer spacing determined by small-angle X-ray scattering is 4.9 nm. These results suggest that each layer shown in the SEM image corresponds to about ten ion conducting layers. The length of monomer **1** in the extended conformation is 2.8 nm, which implies that the polymer forms a bilayer structure.

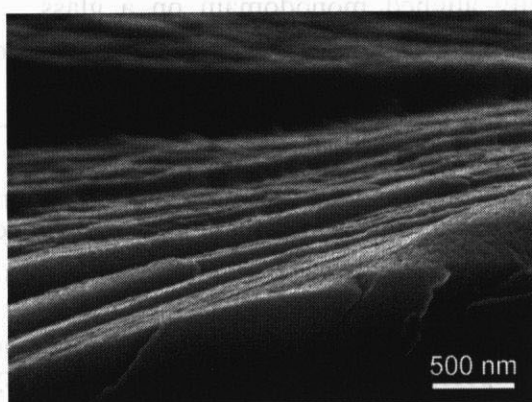


Figure 4-3. SEM picture of the nanostructured film of **poly 1** obtained by in situ photopolymerization of monomer **1** macroscopically aligned in the S_A phase at 58 °C.

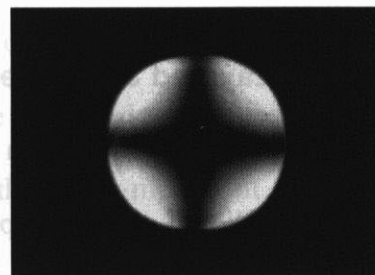


Figure 4-4. Conoscopic figure observed for homeotropically oriented **poly 1** in the solid state at room temperature.

The layered nanostructure of monomer **1** was thermally stabilized by the polymerization. On heating, the film shows a solid- S_A transition at 112 °C and a S_A -isotropic (I) transition at 224 °C. In the solid state and the S_A phase, optically uniaxial conoscopic figures are observed for the oriented films (Figure 4-4), suggesting that the side-chain mesogens form the homeotropic structure in the film.

Ion-Conductive Properties

Ionic conductivities of the polymer film of **poly1** forming the monodomain structure prepared on the glass surface was measured with comb-shaped gold electrodes by an alternating current impedance method. For monomer **1**, its ionic conductivities in the liquid crystalline state could not be obtained because of the monotropic liquid crystalline phase that easily crystallizes during measurements. The in-plane ionic conductivities along the direction parallel to the smectic layer obtained on heating are shown in Figure 4–5 (●). The highest ionic conductivity is $3.2 \times 10^{-2} \text{ S cm}^{-1}$ at 209 °C in the S_A phase. The ionic conductivities decrease at the S_A –Iso phase transition. In contrast, ionic conductivities of **poly1** for the polydomains structure prepared on the ITO surface (○) are below $10^{-3} \text{ S cm}^{-1}$ in the S_A phase (Figure 4–5). At 150 °C, the conductivity of monodomain sample is about 40 times higher than that of the polydomains sample. The boundary in the randomly oriented polydomains disturbs high ion conduction.

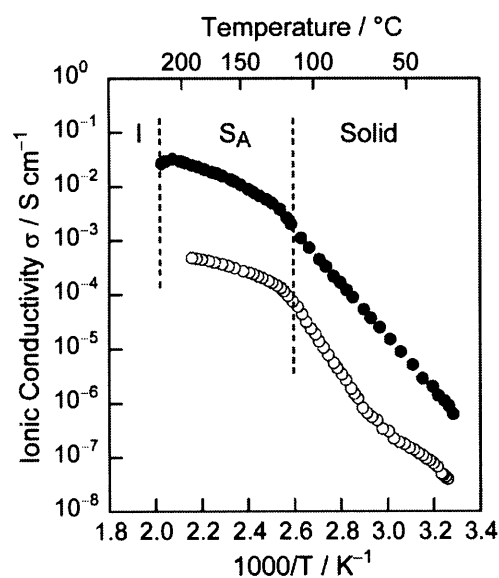


Figure 4–5. Arrhenius plots of ionic conductivities of **poly1** with the uniformly aligned monodomains (●) and **poly1** with unaligned polydomains (○) in the solid state and S_A phases.

As for homeotropically aligned monomer **2** and its polymer **poly2**, ionic conductivities parallel to the layer plane were measured (Figure 4–6). The conductivity of **2** abruptly increases at the Cr–S_{A1} phase transition (82 °C). The polymer **poly2** shows higher ionic conductivity compared to that of **2** below 80 °C. This is due to the formation of polydomain structure of **2** in the crystalline state. In the polymer film of **poly2**, since macroscopically aligned ion-conductive pathways are formed, the conductivity becomes higher than that of **2**.

The improvement of conductive properties was achieved by the photopolymerization of monomer **3** having an oligo(ethylene oxide) spacer (Figure 4–7). This is due to the enhancement of the mobility and dissociation of imidazolium ionic moiety.

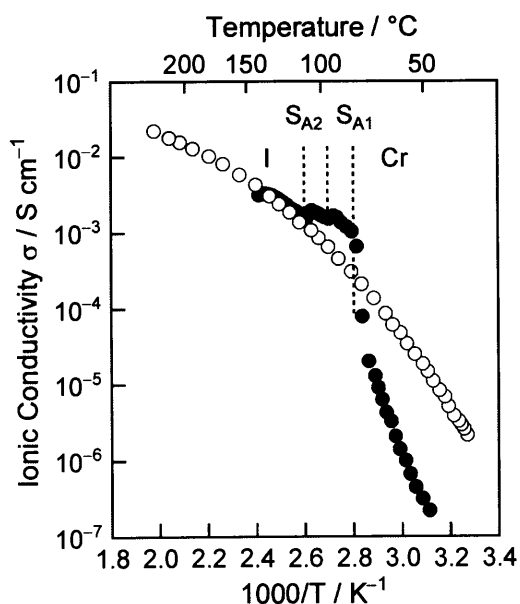


Figure 4–6. Ionic conductivities parallel to the layer of homeotropically aligned **2** (●) and **poly2** (○) as a function of temperature. S_{A1}: semi-bilayer smectic phase with a layer spacing of 3.6 nm; S_{A2}: bilayer smectic phase with a layer spacing of 5.5 nm.

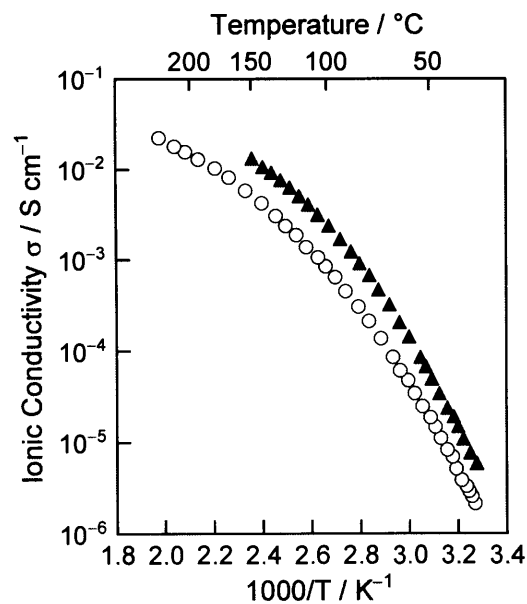


Figure 4–7. Ionic conductivities parallel to the layer of homeotropically aligned **poly3** (▲) and **poly2** (○) as a function of temperature.

These results show that layered nanostructures of ionized side-chain liquid crystalline polymers function as two-dimensional ion-conductors. Previously, functional moieties such as ion- and electro-active moieties were introduced into the side-chain liquid crystalline polymers to induce anisotropic function.³⁴⁻³⁷ For example, a thienyl moiety of the side-chain liquid crystalline polymer was polymerized to give a poly(thiophene) structure.³⁶ However, no macroscopic orientation could be achieved for these pre-organized side-chain polymers because of slow motion and entanglement of polymers. In the present study, the in situ two-dimensional polymerization of oriented self-assembled monomers^{5,37} has shown to be critical to prepare anisotropic ion-conductive films. The use of side-chain liquid crystalline polymers with macroscopically oriented structures is a versatile approach to obtain functional anisotropic self-standing materials.

4.2.2. One-Dimensionally Ion-Conductive Polymer Films

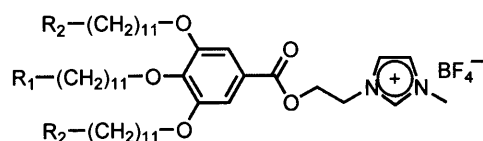
In chapter 2 and 3, columnar liquid crystals based on ionic liquids have been established as new materials for one-dimensional ion transportation. For technical applications, a mechanically stable arrangement of the columnar assembly is necessary. Side-chain liquid crystalline polymers and cross-linked network polymers bearing ion-conductive mesogens were prepared by solution polymerization of ion-conductive monomers.³⁸ These polymers have turned out to be difficult to achieve a macroscopic alignment because of their high viscosity although mechanical orientation was conducted.

In situ photopolymerization of polymerizable columnar liquid crystals³⁹⁻⁴⁴ is a most effective approach to the preparation of columnar network films with a fixed uniform director orientation. Indeed, the fabrication of functional polymer films with macroscopically aligned nanochannels has been realized recently by the photopolymerization of lyotropic columnar liquid crystals.⁴⁵ As the monomers, taper-shaped molecules consisting of a polar head group such as carboxylic and sulfonic acids and a non-polar mesogenic part with three polymerizable groups were designed to form inversed columnar structures in the presence of water. In these systems, nanophase segregation between polar and non-polar parts and intermolecular interactions such as ionic interactions and a hydrogen bonding are driving forces to form such structures. The photopolymerization of the columns aligned vertically on a glass and polymer substrates allowed for preparing nanostructured polymer films that function as nanofilters and catalytic membranes.⁴⁶

In the present study, the author developed one-dimensionally ion-conductive polymer films by in situ photopolymerization of a new columnar liquid crystal bearing an imidazolium ionic moiety. The uniaxial orientation of the column has been achieved by shearing the monomer in the columnar phase. Anisotropic ionic conductivities of the

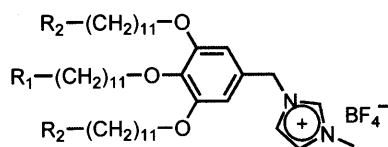
polymers with the fixed unidirectional orientation were measured.

Four polymerizable ionic liquids 4–7 (Figure 4–8) were designed to form columnar liquid crystalline phases at room temperature. Compounds 4 and 5 have a longer spacer between the ionic moiety and tris(alkyloxy)phenyl groups compared to compounds 6 and 7 which are analogues of the columnar ionic liquids without polymerizable groups described in Chapter 3. It is expected that the conductivities of 4 and 5 become higher than those of 6 and 7 because the introduction of the longer spacer enhances the mobility of ionic moieties.



4 : $R_1 = \text{CH}_3$, $R_2 = \text{CH}_2=\text{CH}-\text{COO}$

5 : $R_1 = R_2 = \text{CH}_2=\text{CH}-\text{COO}$



6 : $R_1 = \text{CH}_3$, $R_2 = \text{CH}_2=\text{CH}-\text{COO}$

7 : $R_1 = R_2 = \text{CH}_2=\text{CH}-\text{COO}$

Figure 4–8. Molecular structures of polymerizable ionic liquids.

Liquid Crystalline Properties

Phase transition behavior of synthesized compounds is summarized in Table 4–2. Compound 4 forms a hexagonal columnar liquid crystalline phase between 20 to 50 °C on heating. On the other hand, unfortunately compounds 5–7 do not show non-mesomorphic behavior and become liquids at room temperature. The crystallization temperatures decrease with the increase of the number of polymerizable groups. It was reported that for the liquid

crystalline phthalocyanines, the substitutions (*e.g.* acrylate, and methacrylate groups) at the end of the aliphatic hydrocarbon chains reduce the melting points.⁴⁷ The bulky acrylate moieties at the terminal ends may disturb the packing of alkyl chains. In terms of the linkage between the phenyl ring and imidazolium salt, the use of an ester group for **4** and **5** increases the melting points compared to those of **6** and **7**. This would be due to the increase of the rigidity of molecules.

Table 4–2. Thermal Properties of Compounds 1–4

Compound	phase transition behavior ^a				
4	Cr	20 (44.2)	Col _h	50	I
5	Cr	13 (43.7)			I
6	Cr	5 (34.7)			I
7	Cr	–3 (42.6)			I

^aTransition temperatures (°C) and enthalpies of transition (kJ mol^{–1}, in parentheses) determined by DSC (second heating scan, 10 °C min^{–1}). Col_h: hexagonal columnar; Cr: crystalline; I: isotropic.

In order to examine the columnar structure of monomer **4**, a wide-angle X-ray scattering measurement was performed at 25 °C. Three peaks with the ratio of 1: 1/√3: 1/2 ($d_{100} = 36.2 \text{ \AA}$ at $2\theta = 2.44^\circ$, $d_{110} = 20.8 \text{ \AA}$ at $2\theta = 4.24^\circ$, $d_{200} = 18.1 \text{ \AA}$ at $2\theta = 4.88^\circ$) are seen in the diffraction spectrum. This indicates the formation of a hexagonal columnar structure. The intercolumnar distance (a) is calculated to be 4.17 nm with the following equation: $a = 2\langle d_{100} \rangle / \sqrt{3}$, $\langle d_{100} \rangle = (d_{100} + \sqrt{3}d_{110} + \sqrt{4}d_{200})/3$. Assuming a density of $\rho = 1 \text{ g cm}^{-3}$, the number n of molecules arranged side by side in a single slice of the columns with a thickness (h) of 0.437 nm ($d_{001} = 4.37 \text{ \AA}$ at $2\theta = 20.3^\circ$, a diffuse reflection is assignable to disordered aliphatic chains and the intracolumnar distance) was estimated to be about 4 according to the equation: $n = \sqrt{3}N_A a^2 h \rho / (2M)$, where N_A is the Avogadro's number ($6.02 \times 10^{23} \text{ mol}^{-1}$) and M is the molecular weight ($983.07 \text{ g mol}^{-1}$).⁴⁸ The self-assembly of monomer **4** into the hexagonal columnar structure is illustrated in Figure 4–9. In the hexagonal columnar phase, the salt

moieties should be stabilized into the center of columns.

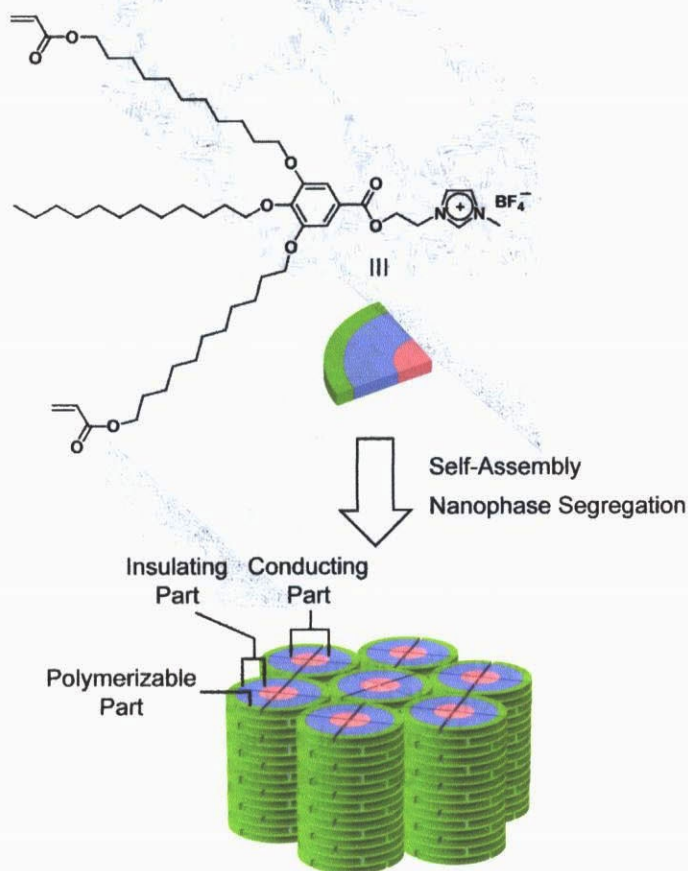


Figure 4-9. Schematic illustration of self-assembly of polymerizable imidazolium salt **4**.

Orientation of Self-Organized Columns

Uniformly homogeneous alignment of the column of monomer **4** was achieved after the polydomain of the columnar phase is sheared in the sandwiched glasses with comb-shaped gold electrodes. Figure 4-10 shows polarizing optical micrographs of **4** in the columnar phase before and after shearing. The direction of the long axis of columns corresponds to the shearing direction, which is confirmed by the periodic change in the pattern with sample's rotation for the polarizing microscopic observation. No birefringence is observed when the shearing direction is along the polarizer or analyzer axis. The highest brightness is seen when the oriented material is in a 45° angle.

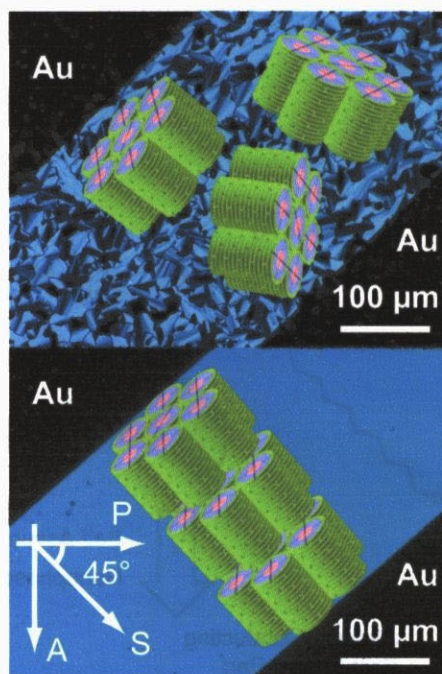


Figure 4–10. Polarizing optical micrographs of monomer **4** and schematic illustrations of the oriented self-assembled columnar structure at 25 °C: (a) before; (b) after shearing the material along the direction perpendicular to the gold electrodes. Directions of A: analyzer; P: polarizer; S: shearing.

Fixation of the Columns by Photopolymerization

Photopolymerization experiments were performed on monomer **4** in the columnar phase at room temperature with 2,2-dimethoxy-2-phenylacetophenone as a photoinitiator. Mechanically stable transparent polymer films as shown in Figure 4–11 were obtained after the UV-irradiation for 60 min.



Figure 4–11. Photograph of the polymer film obtained by photopolymerization of monomer **4** aligned in the columnar phase.

The uniform orientation of the columns of monomer **4** has been successfully preserved by photopolymerization, which was confirmed by polarizing optical microscopic observation. The columnar structure of monomer **4** was stabilized by the polymerization. The polymer film is stable up to at least 300 °C. Wide-angle X-ray diffraction pattern of the polymer film exhibits that a hexagonal columnar structure is retained in the film and the dimensions of the columns slightly increase upon polymerization (Figure 4–12). The intercolumnar distance is 4.33 nm.

In addition, SEM observation was performed for the cross-section of the polymer films to examine the orientation of the films. Figure 4–13 shows that oriented grooves along the direction of shearing were formed in the film.

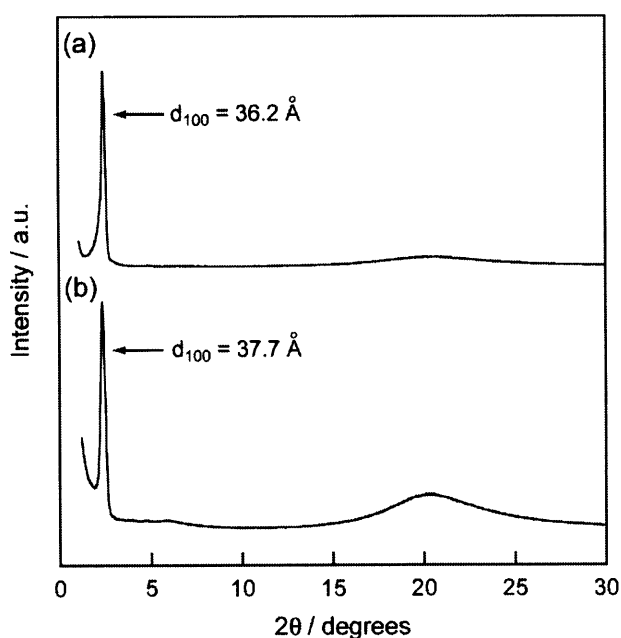


Figure 4–12. X-ray profiles of the hexagonal columnar phase of monomer **4** (a) before polymerization and (b) after polymerization.

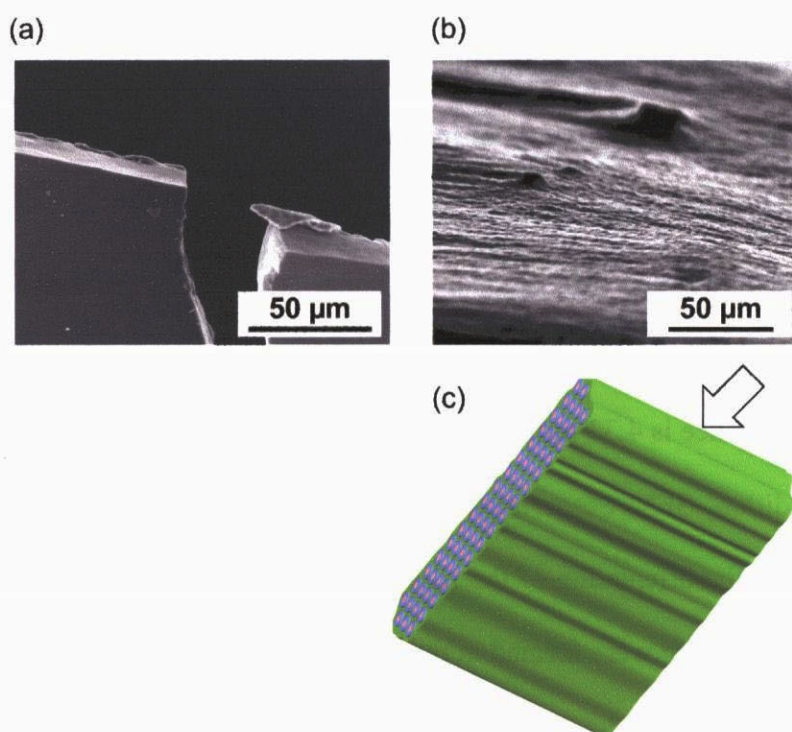


Figure 4–13. FE-SEM images of macroscopically oriented polymer films. (a) over view, (b) edge of the film, and (c) illustration of the polymer film. The arrow indicates the direction of the SEM observation.

Ion-Conductive Properties

Anisotropic ionic conductivities of the oriented monomer **4** and its polymer were measured with comb-shaped gold electrodes by an alternating-current impedance method. Figure 4–14 shows temperature dependence of the ionic conductivities. Both monomer and polymer show anisotropic ionic conductivities. Ionic conductivities parallel (σ_{\parallel}) to the columnar axis are higher than those perpendicular (σ_{\perp}) to the columnar axis. The values of σ_{\parallel} for the monomer is slightly higher than those for the polymer. The magnitude of anisotropy conductivity ($\sigma_{\parallel}/\sigma_{\perp}$) of the polymer is higher than that of the monomer. For example, the monomer shows the conductivities of $3.76 \times 10^{-6} \text{ S cm}^{-1}$ (σ_{\parallel}), $2.44 \times 10^{-7} \text{ S cm}^{-1}$ (σ_{\perp}), and $\sigma_{\parallel}/\sigma_{\perp}$ of 15 at 30 °C. On the other hand, the polymer exhibits the conductivities of $8.50 \times 10^{-5} \text{ S cm}^{-1}$ (σ_{\parallel}), $4.15 \times 10^{-7} \text{ S cm}^{-1}$ (σ_{\perp}), and $\sigma_{\parallel}/\sigma_{\perp}$ of 205 at 73 °C.

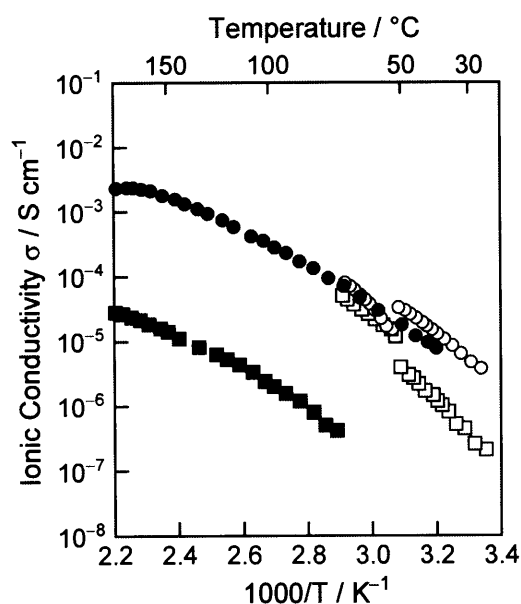


Figure 4–14. Arrhenius plots of ionic conductivities of oriented monomer **4** and its polymer films obtained by photopolymerization of **4**. For the monomer: (○) parallel and (□) perpendicular to the columnar axis. For the polymer: (●) parallel and (■) perpendicular to the columnar axis.

It turned out that the polymerization of the oriented monomer enhanced the anisotropy of conductivities. In the polymer film, cross-linked columns may effectively disturb the ion conduction perpendicular to the columnar axis. Moreover, it is considered that the organized imidazolium salt in the center of columns is in a highly mobile state even after polymerization since no lowering of σ_{\parallel} and no increasing of the activation energy is observed upon polymerization.

Furthermore, in order to examine the effects of nanostructures on ionic conductivities, the author intends to obtain the polydomain polymer film and optically isotropic amorphous polymer film. These polymer films were obtained by photopolymerization of the monomer **4** in the non-oriented columnar phase and in the isotropic phase, respectively. Figure 4–15 shows the ionic conductivities for these polymer films and the oriented polymer films as a function of temperature. For the non-oriented polymer (▲), the value of $1.09 \times 10^{-5} \text{ S cm}^{-1}$ at

100 °C is between the values of σ_{\parallel} ($3.09 \times 10^{-4} \text{ S cm}^{-1}$) and σ_{\perp} ($2.21 \times 10^{-6} \text{ S cm}^{-1}$) for the oriented film at the same temperature. As for the isotropic film (∇), the value of $3.68 \times 10^{-5} \text{ S cm}^{-1}$ at 100 °C is lower than that of σ_{\parallel} for the oriented film at the same temperature and is higher than that of the non-oriented film. These results indicate that the introduction of oriented nanostructure enhances the conductivity of the polymer film. The improvement in ionic conductivities is not achieved when the nanostructure is not aligned macroscopically.

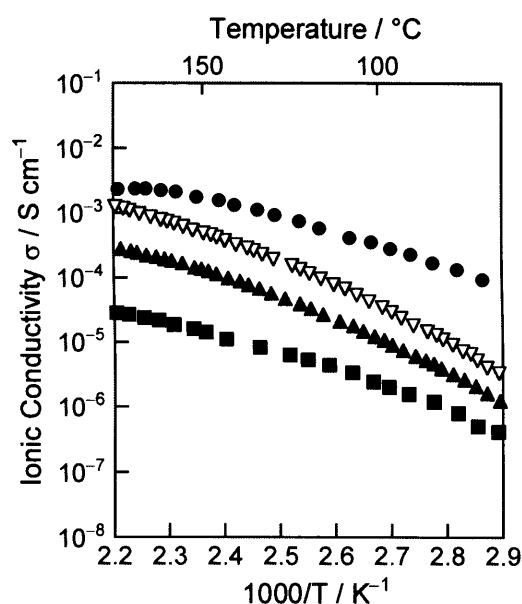


Figure 4–15. Ionic conductivities of the polymer films obtained by photopolymerization of **4** in the columnar state at room temperature and in the isotropic state at 60 °C: (●) parallel and (■) perpendicular to the columnar axis for the aligned film; (▲) non-oriented polymer film with polydomain structures; (▽) optically isotropic amorphous film.

4.3. Conclusions

Two-dimensionally ion-conductive polymer films were obtained by photopolymerization of smectic liquid crystalline monomers containing an imidazolium tetrafluoroborate salt. The ionic conductivities parallel to the layer plane are higher than those of polydomain structures. The improvement of conductivities is achieved by the introduction of an oligo(ethylene oxide) chain as a spacer between the salt moiety and biphenyl mesogen.

A one-dimensionally ion-conductive polymer film was also prepared by fixation of the oriented columnar ionic liquid crystalline monomer. The oriented polymer film showed higher ionic conductivities compared to the non-oriented polymer film and isotropic amorphous film. For the improvement of conductive properties, it is essential to control the orientation of the nanostructure. This oriented columnar film should be useful for polymer electrolyte batteries, catalytic membranes, nanofiltration membranes, and so on.

4.4. Experimental

General Methods. All reagents were purchased from Aldrich and Tokyo Kasei and used as received. All of the reactions were carried out under an argon atmosphere in a dry solvent purchased from Kanto Chemicals. All reactions were carried out under argon atmosphere. Analytical thin layer chromatography (TLC) was performed on silica gel plates of E. Merck (Silica Gel F254). Flash chromatography was carried out with silica gel 60 (spherical 40-50 μm). Recycling preparative GPC was carried out with a Japan Analytical Industry LC-908 chromatograph. ^1H NMR and ^{13}C NMR spectra were obtained using a JEOL JNM-LA400 at 400 and 100 MHz in CDCl_3 , respectively. Chemical shifts of ^1H and ^{13}C NMR signals were quoted to $(\text{CH}_3)_4\text{Si}$ ($\delta = 0.00$) and CDCl_3 ($\delta = 77.0$) as internal standards, respectively, and expressed by chemical shifts in ppm (δ), multiplicity, coupling constant (Hz), and relative

intensity. Elemental analyses were carried out on a Perkin-Elmer CHNS/O 2400 apparatus. UV irradiation was carried out by using a high pressure mercury lamp (Ushio, 500 W) with appropriate glass filter (Asahi Technoglass UV-35 and UVD-36C) as an irradiation source. IR measurements were conducted on a JASCO FT/IR-660 Plus spectrometer equipped with a JASCO IRT-30 microscope to confirm the polymerization of monomers.

Characterization of Phase Transition Behavior. Differential scanning calorimetry (DSC) measurements were performed with a NETZSCH DSC204 *Phoenix*[®] at a scanning rate of 5 °C min⁻¹. The transition temperatures were taken at the maximum point of exothermic and the minimum point of endothermic peaks, respectively. A polarizing optical microscope Olympus BH-2 equipped with a Mettler FP82 HT hot-stage was used for visual observation. Wide-angle X-ray diffraction (WAXD) patterns were obtained using a Rigaku RINT-2100 system with monochromated CuK α radiation.

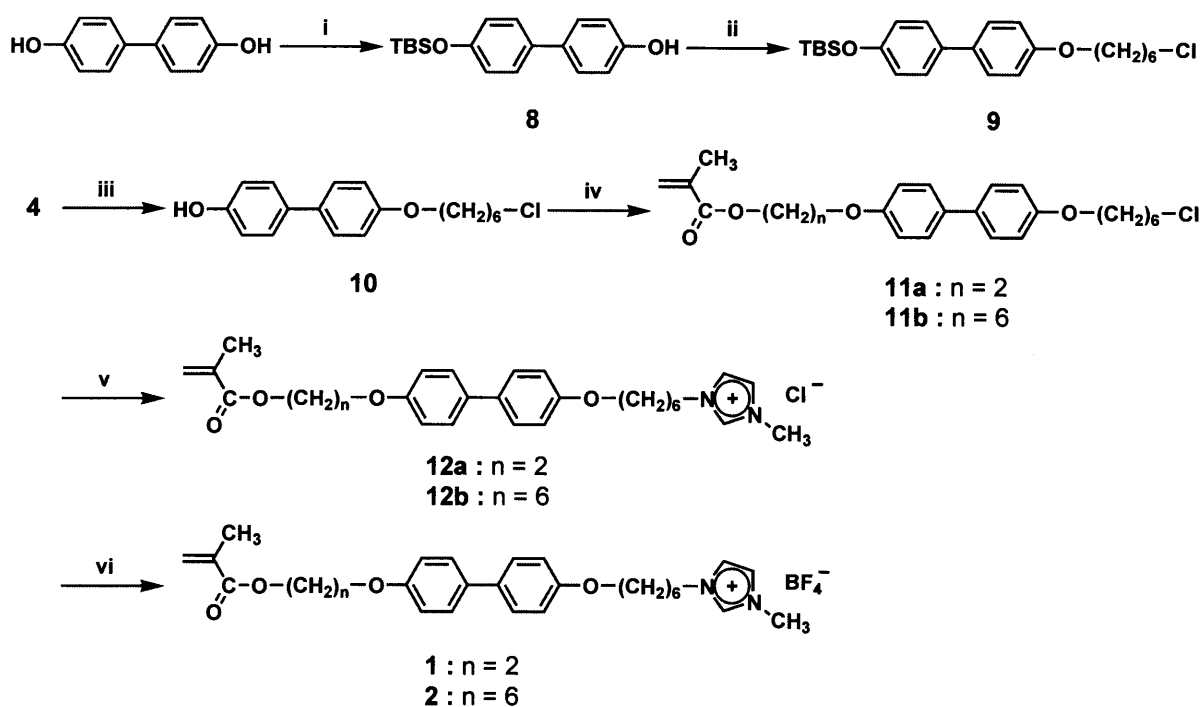
Sample Preparation and In Situ Photopolymerization. After the addition of a dichloromethane solution of 2,2-dimethoxy-2-phenylacetophenone as a photoinitiator to monomers (0.5 wt % to monomers), the solvent was evaporated and dried under reduced pressure at room temperature. All processes were carried out in dark condition to prevent unwanted photopolymerization during the preparation. The polymerizable sample was sandwiched between two glass substrates and heated to the isotropic states. Then, the sample was cooled to the liquid crystalline states at a rate of 1 °C min⁻¹. Monomers **1–3** in the S_A phases spontaneously form homeotropic monodomains on the surface of the glass substrate and polydomains on the ITO substrate. As for monomer **4**, macroscopically homogeneous alignment of columnar structure was achieved by shearing the materials in the Col_h phase.

Photopolymerization of the monomers in the liquid crystalline phases was carried out under the exposure to UV light (365 nm, 22 mW/cm²) for 15–60 min.

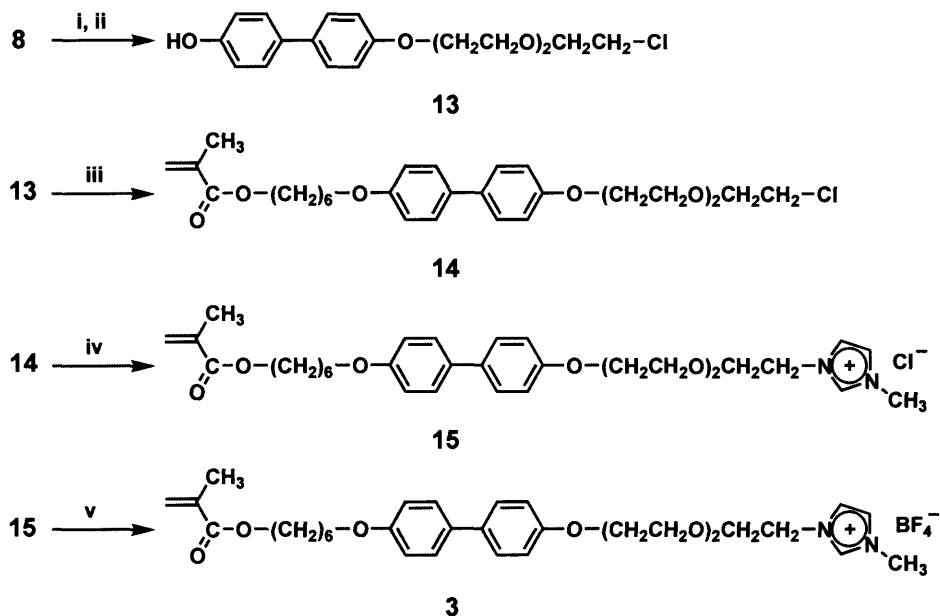
FE-SEM Observation. High resolution scanning electron microscopy measurements were performed on a HITACHI S-900 at an accelerating voltage of 10 kV for the nanostructured polymer film. The naked films were obtained by peeling off from glass substrates. The resultant films were shaded with platinum and used for FE-SEM observation.

Measurements of Ionic Conductivities. Ionic conductivities were measured by the alternating current impedance method using a Schlumberger Solartron 1260 impedance analyzer (frequency range: 10 Hz–10 MHz, applied voltage: 0.3 V) and a temperature controller. The heating rate of the measurements was fixed to 3 °C min⁻¹ from 30 to 200 °C. Ionic conductivities were calibrated with aq. KCl solution (1.00 mmol L⁻¹) as a standard conductive solution. Two types of cells with gold and indium tin oxide (ITO) electrodes were used to measure ionic conductivities for uniformly and randomly oriented layered films, respectively.

Synthesis of smectic liquid crystalline monomers. Monomers **1** and **2** were synthesized by following the procedures shown in scheme 4–1. Monomer **3** was also prepared by the similar method (scheme 4–2). The methylene or ethylene oxide spacer and the polymerizable groups were attached to a mesogenic biphenyl core by Mitsunobu etherification reactions.⁴⁹ Imidazolium chloride salts were obtained by the reactions of the resultant compounds having a methylene chloride and 1-methylimidazole, followed by ion-exchange reaction using silver tetrafluoroborate.



Scheme 4–1. Synthetic procedure of monomers **1** and **2**. i) TBSCl, imidazole, DMF; ii) 6-chloro-1-hexanol, DEAD, PPh₃, toluene; iii) TBAF, CH₂Cl₂; iv) 2-hydroxyethyl methacrylate or 6-hydroxyhexyl methacrylate, DEAD, PPh₃, toluene; v) 1-methylimidazole, 45 °C; vi) AgBF₄, methanol.



Scheme 4-2. Synthetic procedure of monomer **3**.

i) 2-{2-(2-chloroethoxy)ethoxy}ethanol, DEAD, PPh₃, toluene; ii) TBAF, CH₂Cl₂; iii) 6-hydroxyhexyl methacrylate, DEAD, PPh₃, toluene; iv) 1-methylimidazole, 45 °C; v) AgBF₄, methanol.

4-*tert*-Butyldimethylsilyloxy-4'-hydroxy-1,1'-biphenyl (8). Compound **8** was prepared by the reaction of excess 4,4'-biphenol with *tert*-butyldimethylsilyl chloride (TBSCl) in a *N,N*-dimethylformamide (DMF) solution in the presence of imidazole as already reported.¹⁸ ¹H NMR (400 MHz): $\delta = 7.42$ (d, $J = 8.8$ Hz, 2H), 7.40 (d, $J = 8.8$ Hz, 2H), 6.89 (d, $J = 8.8$ Hz, 2H), 6.88 (d, $J = 8.8$ Hz, 2H), 5.58 (s, 1H), 1.00 (s, 9H), 0.22 (s, 6H). ¹³C NMR (100 MHz): $\delta = 154.7, 154.5, 133.9, 133.7, 127.9, 127.6, 120.3, 115.5, 25.7, 18.2, -4.4$. IR (KBr): 3273, 2956, 2930, 2857, 1607, 1500, 1458, 1243, 1170, 911, 840, 822, 781 cm⁻¹. Melting point: 97 °C.

4-tert-Butyldimethylsilyloxy-4'-(6-chlorohexyloxy)-1,1'-biphenyl (9). To a solution of triphenylphosphine (PPh₃) (13.6 g, 52 mmol), 6-chloro-1-hexanol (7.2 g, 52 mmol), and **8** (12.3 g, 41 mmol) in toluene (50 mL), diethyl azodicarboxylate (DEAD) (8.5 mL, 52 mmol) was slowly added dropwise with stirring. After the mixture was stirred at room temperature for 3 d, the resulting mixture was poured into water (200 mL) and a sat. NH₄Cl aqueous solution (20 mL). The organic materials were dissolved in ethyl acetate (200 mL) and the organic phase was separated. The aqueous phase was extracted with ethyl acetate four times. The combined organic phase was washed with a sat. NaCl aqueous solution, dried over anhydrous MgSO₄, filtered through a pad of Celite, and concentrated *in vacuo*. The crude product was purified by flash column chromatography on silica gel (eluent: hexane/chloroform = 5/1 followed by hexane/chloroform = 1/1) to give **9** (15.3 g, 38 mmol) in a yield of 91 % as a white powder. ¹H NMR (400 MHz): δ = 7.46 (d, *J* = 8.8 Hz, 2H), 7.41 (d, *J* = 8.8 Hz, 2H), 6.94 (d, *J* = 8.8 Hz, 2H), 6.88 (d, *J* = 8.8 Hz, 2H), 3.99 (t, *J* = 6.8 Hz, 2H), 3.56 (t, *J* = 6.8, 2H), 1.82 (m, 4H), 1.52 (t, *J* = 6.8 Hz, 4H), 1.00 (s, 9H), 0.22 (s, 6H). ¹³C NMR (100 MHz): δ = 158.1, 154.7, 134.0, 133.4, 127.7, 127.6, 120.3, 114.7, 67.8, 45.0, 32.5, 29.1, 26.6, 25.7, 25.4, 18.2, -4.4. IR (KBr): 3033, 2931, 2859, 1891, 1605, 1496, 1471, 1390, 1362, 1252, 1168, 1114, 829, 731, 679 cm⁻¹. Elemental analysis calcd. (%) for C₂₄H₃₅ClO₂Si: C, 68.78; H, 8.42. Found: C, 69.11; H, 8.21. Melting point: 52 °C.

4-(6-Chlorohexyloxy)-4'-hydroxy-1,1'-biphenyl (10). After a solution of tetra-*n*-butylammonium fluoride (1.02 g, 4.7 mmol) in CH₂Cl₂ (20 mL) was slowly added to a solution of **9** (1.03 g, 2.5 mmol) in CH₂Cl₂ (30 mL) with stirring, the mixture was stirred at room temperature for 1 d. The resulting mixture was poured into water (100 mL), and extracted with chloroform three times. The organic extracts were washed with a sat. NaCl

aqueous solution, dried over anhydrous MgSO_4 , filtered, and concentrated *in vacuo*. The residue was purified by flash column chromatography on silica gel (eluent: chloroform followed by chloroform/methanol = 10/1) to give **10** (0.69 g, 2.3 mmol) in a yield of 90 % as a colorless powder. ^1H NMR (400 MHz): δ = 7.45 (d, J = 8.8 Hz, 2 H), 7.43 (d, J = 8.8 Hz, 2 H), 6.94 (d, J = 8.8 Hz, 2 H), 6.88 (d, J = 8.8 Hz, 2 H), 4.73 (s, 1 H), 4.00 (t, J = 6.8 Hz, 2 H), 3.56 (t, J = 6.8 Hz, 2 H), 1.82 (m, 4 H), 1.52 (t, J = 6.8 Hz, 4 H). ^{13}C NMR (100 MHz): δ = 158.2, 154.6, 133.7, 133.3, 127.9, 127.7, 115.6, 114.7, 67.8, 45.0, 32.5, 29.1, 26.7, 25.4. IR (KBr): 3380, 3065, 2998, 2933, 2864, 1885, 1614, 1505, 1462, 1351, 1256, 1195, 1178, 1136, 816, 728, 707 cm^{-1} . Elemental analysis calcd. (%) for $\text{C}_{18}\text{H}_{21}\text{ClO}_2$: C, 70.93; H, 6.94. Found: C, 71.07; H, 6.94. Melting point: 130 °C.

4-(6-Chlorohexyloxy)-4'-(2-methacryloyloxyethoxy)-1,1'-biphenyl (11a). DEAD (2.0 mL, 12.7 mmol) was added dropwise to a suspension of PPh_3 (3.6 g, 13.6 mmol), **10** (3.0 g, 9.9 mmol), and 2-hydroxyethyl methacrylate (HEMA) (1.68 g, 12.9 mmol) in toluene (40 mL) with stirring at 0 °C. The mixture was stirred at room temperature in the dark for 5 h. The resulting mixture was poured into water (100 mL) and a sat. NH_4Cl aqueous solution (10 mL) and extracted with ethyl acetate three times. The combined organic extracts were washed with a sat. NaCl aqueous solution, dried over anhydrous MgSO_4 , filtered, and concentrated *in vacuo*. The crude product was purified by flash column chromatography on silica gel (eluent: hexane/chloroform = 1/1) to give **11a** (3.1 g, 7.5 mmol) in a yield of 76 % as a white powder. ^1H NMR (400 MHz): δ = 7.47 (d, J = 8.8 Hz, 2 H), 7.46 (d, J = 8.8 Hz, 2 H), 6.97 (d, J = 8.8 Hz, 2 H), 6.94 (d, J = 8.8 Hz, 2 H), 6.15 (s, 1 H), 5.59 (s, 1 H), 4.51 (t, J = 4.9 Hz, 2 H), 4.25 (t, J = 4.9 Hz, 2 H), 3.99 (t, J = 6.8 Hz, 2 H), 3.56 (t, J = 6.8 Hz, 2 H), 1.96 (s, 3 H), 1.82 (m, 4 H), 1.52 (t, J = 6.8 Hz, 4 H). ^{13}C NMR (100 MHz): δ = 167.3, 158.2, 157.6, 136.0, 134.0,

133.2, 127.7, 127.7, 126.1, 114.9, 114.7, 67.8, 66.0, 63.1, 45.0, 32.5, 29.1, 26.6, 25.4, 18.3. IR (KBr): 3072, 3044, 2932, 1890, 1870, 1717, 1637, 1606, 1502, 1453, 1407, 1386, 1325, 1271, 1180, 1065, 898, 827 cm^{-1} . Elemental analysis calcd. (%) for $\text{C}_{24}\text{H}_{29}\text{ClO}_4$: C, 69.14; H, 7.01. Found: C, 69.12; H, 7.01. Melting point: 82 °C.

4-(6-Chlorohexyloxy)-4'-(6-methacryloyloxyethoxy)-1,1'-biphenyl (11b). DEAD (1.3 mL, 8.3 mmol) was added dropwise to a suspension of PPh_3 (2.2 g, 8.2 mmol), **10** (2.0 g, 6.7 mmol), 6-hydroxyhexyl methacrylate (1.50 g, 8.0 mmol), 2,6-di-*tert*-butylphenol (56 mg, 0.27 mmol) in toluene (30 mL) with stirring at 0 °C. The mixture was stirred at room temperature in the dark for 22 h. The resulting mixture was poured into water (100 mL) and a sat. NH_4Cl aqueous solution (100 mL) and extracted with ethyl acetate three times. The combined organic extracts were washed with a sat. NaCl aqueous solution, dried over anhydrous MgSO_4 , filtered, and concentrated *in vacuo*. The crude product was purified by flash column chromatography on silica gel (eluent: chloroform) to give **11b** (2.3 g, 4.8 mmol) in a yield of 72 % as a white powder. ^1H NMR (400 MHz): δ = 7.46 (d, J = 8.8 Hz, 4H), 6.94 (d, J = 8.8 Hz, 4H), 6.11 (s, 1H), 5.55 (s, 1H), 4.16 (t, J = 6.8 Hz, 2H), 4.00 (t, J = 6.3 Hz, 4H), 3.56 (t, J = 6.8 Hz, 2H), 1.95 (s, 3H), 1.90–1.77 (m, 6H), 1.73 (tt, J = 7.3, 6.8 Hz, 2H), 1.61–1.45 (m, 8H).

1-Methyl-3-((4-(2-methacryloyloxyethoxy)-1,1'-biphenyl-4'-oxy)hexyl)imidazolium chloride (12a). A mixture of **11a** (3.1 g, 7.5 mmol), 2,6-di-*tert*-butylphenol (0.80 g, 3.9 mmol), and excess 1-methylimidazole (7.1 g, 87 mmol) was stirred at 45 °C for 17 h in a light resistant container. The crude product was purified by flash column chromatography on silica gel (eluent: chloroform/methanol = 5/1 followed by 4/1) to give **12a** (1.25 g, 2.5 mmol) in a

yield of 34 % as a white powder. ^1H NMR (400 MHz): δ = 11.17 (s, 1 H), 7.47 (d, J = 8.8 Hz, 2 H), 7.46 (d, J = 8.8 Hz, 2 H), 7.16 (s, 1 H), 7.16 (s, 1 H), 6.98 (d, J = 8.8 Hz, 2 H), 6.93 (d, J = 8.8 Hz, 2 H), 6.15 (s, 1 H), 5.60 (s, 1 H), 4.52 (t, J = 4.9 Hz, 2 H), 4.36 (t, J = 7.3 Hz, 2 H), 4.26 (t, J = 4.9 Hz, 2 H), 4.11 (s, 3 H), 3.99 (t, J = 6.3 Hz, 2 H), 1.97 (m, 2 H), 1.96 (s, 3 H), 1.81 (m, 2 H), 1.56 (m, 2 H), 1.45 (m, 2 H). ^{13}C NMR (100 MHz): δ = 167.2, 158.0, 157.5, 137.9, 135.8, 133.7, 133.1, 127.6, 127.6, 126.0, 123.3, 121.7, 114.9, 114.6, 67.5, 66.0, 63.0, 49.8, 36.5, 30.1, 28.8, 25.8, 25.4, 18.2. Phase transition temperatures ($^{\circ}\text{C}$): Iso 76 S_X 44 Cr, Iso = isotropic, S_X = unidentified smectic, Cr = crystalline (DSC on cooling).

1-Methyl-3-((4-(6-methacryloyloxyhexyloxy)-1,1'-biphenyl-4'-oxy)hexyl)imidazolium chloride (12b). A mixture of **11b** (3.00 g, 6.34 mmol), 2,6-di-*tert*-butylphenol (62 mg, 0.30 mmol), and 1-methylimidazole (4.50 g, 54.8 mmol) was stirred at 40 $^{\circ}\text{C}$ for 18 h in a light resistant container. The crude product was purified by flash column chromatography on silica gel (eluent: chloroform/methanol = 5/1 followed by 4/1) to give **12b** (2.43 g, 4.38 mmol) in a yield of 34 % as a white powder.

1-Methyl-3-((4-(2-methacryloyloxyethoxy)-1,1'-biphenyl-4'-oxy)hexyl)imidazolium tetrafluoroborate (1). A solution of silver tetrafluoroborate (0.23 g, 1.20 mmol) in methanol (10 mL) was added dropwise to a solution of **12a** (0.46 g, 0.93 mmol) in methanol with stirring at 0 $^{\circ}\text{C}$. The mixture was stirred at room temperature in the dark for 2 h. An insoluble material was removed through a suction funnel, and the solution was concentrated *in vacuo*. The residue was purified by flash column chromatography on silica gel (eluent: chloroform/methanol = 5/1) to give **1** (0.107 g, 0.195 mmol) in a yield of 94 % as a white powder. ^1H NMR (400 MHz): δ = 8.77 (s, 1 H), 7.46 (d, J = 8.3 Hz, 2 H), 7.44 (d, J = 8.8 Hz,

2 H), 7.28 (s, 1 H), 7.25 (s, 1 H), 6.96 (d, $J = 8.3$ Hz, 2 H), 6.92 (d, $J = 8.8$ Hz, 2 H), 6.15 (s, 1 H), 5.59 (s, 1 H), 4.50 (t, $J = 4.9$ Hz, 2 H), 4.24 (t, $J = 4.9$ Hz, 2 H), 4.16 (t, $J = 7.3$ Hz, 2 H), 3.96 (t, $J = 6.3$ Hz, 2 H), 3.91 (s, 3H), 1.95 (s, 3H), 1.89 (m, 2 H), 1.77 (m, 2 H), 1.51 (m, 2 H), 1.41 (m, 2 H). ^{13}C NMR (100 MHz): $\delta = 167.4, 158.2, 157.7, 136.5, 136.0, 133.9, 133.2, 127.7, 127.7, 126.1, 123.5, 122.0, 115.0, 114.8, 67.6, 66.1, 63.1, 50.0, 36.3, 29.9, 28.9, 25.8, 25.4, 18.3$. IR (KBr): 3157, 3102, 2938, 2865, 1719, 1634, 1606, 1568, 1500, 1470, 1455, 1300, 1273, 1252, 1177, 1065, 1055, 826, 808 cm^{-1} . Elemental analysis calcd. (%) for $\text{C}_{28}\text{H}_{35}\text{BF}_4\text{N}_2\text{O}_4$: C, 61.10; H, 6.41; N, 5.09. Found: C, 61.25; H, 6.43; N, 5.24. Phase transition temperatures ($^{\circ}\text{C}$): Iso 60 S_A 52 S_{X1} 49 S_{X2} 39 Cr, $S_A =$ smectic A, $S_{X1}, S_{X2} =$ unidentified smectic (DSC on cooling).

1-Methyl-3-((4-(6-methacryloyloxyhexyloxy)-1,1'-biphenyl-4'-oxy)hexyl)imidazolium tetrafluoroborate (2). A solution of silver tetrafluoroborate (0.779 g, 4.00 mmol) in methanol (10 mL) was added dropwise to a solution of **12b** (1.82 g, 3.28 mmol) in methanol with stirring at room temperature. The mixture was stirred at room temperature in the dark for 2 h. An insoluble material was removed through a suction funnel, and the solution was concentrated *in vacuo*. The residue was purified by flash column chromatography on silica gel (eluent: chloroform/methanol = 5/1) followed by GPC to give **2** (1.92 g, 3.17 mmol) in a yield of 97 % as a white powder. ^1H NMR (400 MHz): $\delta = 8.82$ (s, 1H), 7.45 (d, $J = 8.8$ Hz, 4H), 7.31 (s, 1H), 7.28 (s, 1H), 6.92 (d, $J = 8.8$ Hz, 2H), 6.91 (d, $J = 8.8$ Hz, 2H), 6.10 (s, 1H), 5.55 (s, 1H), 4.16 (t, $J = 6.8$ Hz, 4H), 3.97 (t, $J = 6.3$ Hz, 2H), 3.94 (t, $J = 6.3$ Hz, 2H), 3.90 (s, 3H), 1.94 (s, 3H), 1.94–1.67 (m, 8H), 1.62–1.33 (m, 8H). ^{13}C NMR (100 MHz): $\delta = 167.5, 158.1, 158.0, 136.4, 136.3, 133.2, 133.1, 127.5, 125.2, 123.5, 122.0, 114.7, 67.8, 67.5, 64.6, 49.8, 36.2, 29.8, 29.1, 28.8, 28.5, 25.8, 25.7, 25.3, 18.3$. IR (KBr): 3141, 3060, 3010, 2942, 2865,

1708, 1635, 1608, 1569, 1504, 1474, 1405, 1325, 1300, 1276, 1252, 1176, 1169, 1123, 1084, 1063, 1037, 995, 949, 935, 824, 801 cm^{-1} . Elemental analysis calcd. (%) for $\text{C}_{32}\text{H}_{43}\text{ClN}_2\text{O}_4$: C, 69.23; H, 7.81; N, 5.05. Found: C, 69.03; H, 7.62; N, 5.31. Phase transition temperatures ($^{\circ}\text{C}$): Iso 106 $\text{S}_{\text{A}2}$ 93 $\text{S}_{\text{A}1}$ 35 Cr (DSC on cooling).

4-(2-(2-(2-Chloroethoxy)ethoxy)ethoxy)-4'-hydroxy-1,1'-biphenyl (13). To a solution of triphenylphosphine (PPh_3) (2.36 g, 9.00 mmol), 2-(2-(2-chloroethoxy)ethoxy)ethanol (1.52 g, 9.00 mmol), and **8** (2.58 g, 8.59 mmol) in toluene (50 mL), diethyl azodicarboxylate (DEAD) (1.42 mL, 9.00 mmol) was slowly added dropwise with stirring. After the mixture was stirred for 10 h at room temperature, the resulting mixture was poured into water (100 mL) and a sat. NH_4Cl aqueous solution (100 mL). The organic materials were dissolved in ethyl acetate (200 mL) and the organic phase was separated. The aqueous phase was extracted with ethyl acetate three times. The combined organic phase was washed with a sat. NaCl aqueous solution, dried over anhydrous MgSO_4 , filtered through a pad of Celite, and concentrated *in vacuo*. The crude product was purified by flash column chromatography on silica gel (eluent: hexane/chloroform = 5/1) to give 4-*tert*-butyldimethylsilyloxy-4'-(2-(2-(2-chloroethoxy)ethoxy)ethoxy)-1,1'-biphenyl as a pale yellow liquid. Tetra-*n*-butylammonium fluoride (0.92 g, 3.52 mmol) in CH_2Cl_2 (10 mL) was slowly added to the solution of the TBS-protected compound in CH_2Cl_2 (20 mL). The mixture was stirred at room temperature for 8 h. The resulting mixture was poured into water (100 mL), and extracted with chloroform three times. The organic extracts were washed with a sat. NaCl aqueous solution, dried over anhydrous MgSO_4 , filtered, and concentrated *in vacuo*. The residue was purified by flash column chromatography on silica gel (eluent: chloroform followed by chloroform/methanol = 10/1) to give **13** (2.07 g, 6.15 mmol) in a yield of 72 % as

a white solid. ^1H NMR (400 MHz): δ = 7.41 (d, J = 8.8 Hz, 2H), 7.37 (d, J = 8.8 Hz, 2H), 6.92 (d, J = 8.8 Hz, 2H), 6.87 (d, J = 8.8 Hz, 2H), 5.42 (s, 1H), 4.14 (t, J = 4.4 Hz, 2H), 3.89 (t, J = 4.8, 2H), 3.80–3.73 (m, 6H), 3.64 (t, J = 6 Hz, 2H). ^{13}C NMR (100 MHz): δ = 157.7, 154.8, 133.56, 133.33, 127.84, 127.59, 115.60, 114.78, 100.51, 71.38, 70.75, 70.66, 69.85, 67.35, 42.66. IR (KBr): 3261, 2929, 2885, 1607, 1590, 1502, 1450, 1355, 1274, 1246, 1220, 1173, 1138, 1110, 1063, 947, 920, 826, 669 cm^{-1} . Elemental analysis calcd. (%) for $\text{C}_{18}\text{H}_{21}\text{ClO}_4$: C, 64.19; H, 6.28. Found: C, 64.31; H, 6.28.

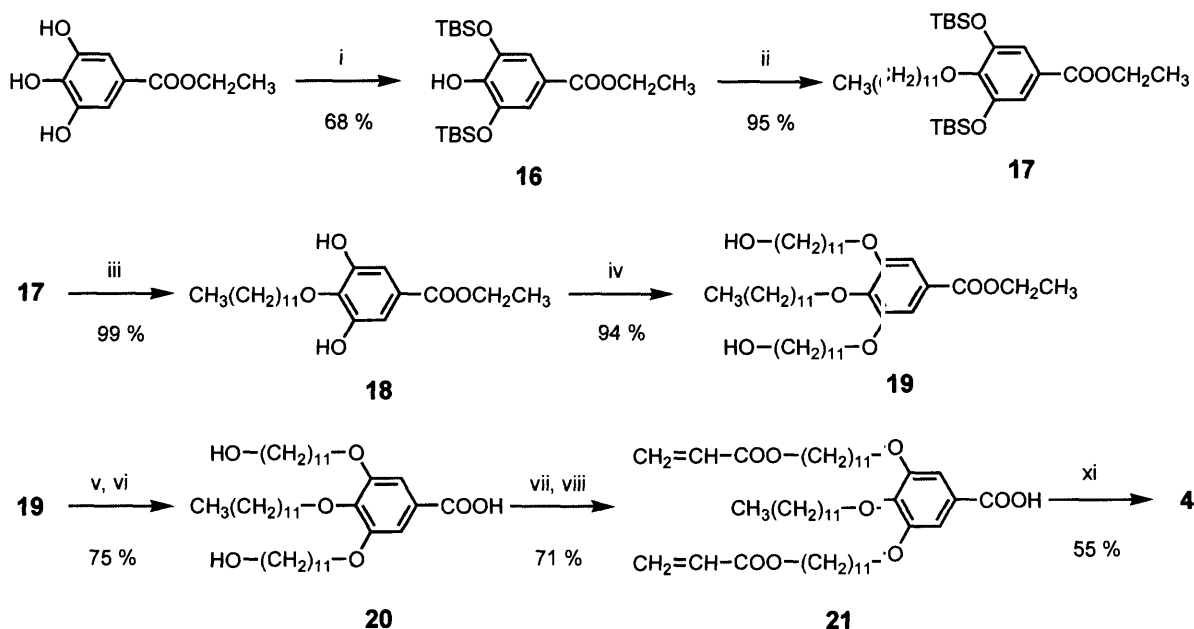
4-(2-(2-(2-Chloroethoxy)ethoxy)ethoxy)-4'-(6-methacryloyloxyhexyloxy)-1,1'-biphenyl (14). Yield 86 %. White solid. ^1H NMR (400 MHz): δ = 7.46 (dd, J = 8.8, 0.8 Hz, 4H), 6.97 (d, J = 8.8 Hz, 2H), 6.93 (d, J = 8.8 Hz, 2H), 6.10 (s, 1H), 5.55 (t, J = 1.2 Hz, 1H), 4.18–4.14 (m, 4H), 3.99 (t, J = 6.4 Hz, 2H), 3.89 (t, J = 4.8 Hz, 2H), 3.79–3.70 (m, 6H), 3.64 (t, J = 5.6 Hz, 2H), 1.94 (s, 1H), 1.82 (t, J = 6.8 Hz, 2H), 1.72 (t, J = 7.2 Hz, 2H), 1.53–1.46 (m, 4H). ^{13}C NMR (100 MHz): δ = 167.50, 158.14, 157.79, 136.44, 133.64, 133.20, 127.63, 127.61, 125.21, 114.82, 114.67, 71.36, 70.80, 70.67, 69.81, 67.79, 67.45, 64.62, 42.71, 29.15, 28.52, 25.78, 25.74, 18.32. IR (KBr): 2934, 2885, 2861, 1717, 1637, 1568, 1501, 1470, 1455, 1389, 1373, 1358, 1321, 1295, 1269, 1244, 1164, 1132, 1109, 1075, 1060, 1044, 986, 934, 850, 826, 802, 658 cm^{-1} . Elemental analysis calcd. (%) for $\text{C}_{28}\text{H}_{37}\text{ClO}_6$: C, 66.59; H, 7.38. Found: C, 66.52; H, 7.38.

1-Methyl-3-(2-(2-(2-(4-(6-methacryloyloxyhexyloxy)-1,1'-biphenyl-4'-oxy)ethoxy)ethoxy)ethyl)imidazolium chloride (15). Yield 86 %. White solid. ^1H NMR (400 MHz): δ = 10.14 (s, 1H), 7.37 (s, 1H), 7.47 (d, J = 6.8 Hz, 2H), 7.45 (d, J = 6.8 Hz, 2H), 7.29 (s, 1H), 7.08 (s, 1H), 6.94 (d, J = 8.0 Hz, 4H), 6.10 (s, 1H), 5.55 (s, 1H), 4.59 (t, J = 4.4 Hz, 2H),

4.18–4.14 (m, 4H), 3.99 (t, $J = 6.4$ Hz, 2H), 3.95 (s, 1H), 3.89 (t, $J = 4.8$ Hz, 2H), 3.85 (t, $J = 4.4$, 2H), 3.69 (m, 4H), 2.78 (s, 4H), 1.94 (s, 3H), 1.55–1.45 (m, 8H). ^{13}C NMR (100 MHz): $\delta = 167.47, 158.20, 157.60, 137.81, 136.37, 133.77, 132.82, 127.64, 127.52, 125.20, 123.39, 122.34, 114.75, 114.70, 70.27, 70.10, 69.56, 69.04, 67.77, 67.47, 64.57, 49.51, 36.34, 29.08, 28.46, 25.71, 25.67, 18.25$. IR (KBr): 3087, 2935, 1717, 1604, 1559, 1500, 1471, 1455, 1389, 1363, 1323, 1297, 1270, 1244, 1169, 1138, 1101, 1065, 987, 955, 929, 825 cm^{-1} . Elemental analysis calcd. (%) for $\text{C}_{32}\text{H}_{43}\text{ClN}_2\text{O}_6$: C, 65.46; H, 7.38; N, 4.77. Found: C, 65.61; H, 7.31; N, 4.81.

1-Methyl-3-(2-(2-(2-(4-(6-methacryloyloxyhexyloxy)-1,1'-biphenyl-4'-oxy)ethoxy)ethoxy)ethyl)imidazolium tetrafluoroborate (3). Yield 64 %. White solid. ^1H NMR (400 MHz): $\delta = 9.06$ (s, 1H), 7.50 (s, 1H), 7.48 (d, $J = 6.8$ Hz, 2H), 7.43 (d, $J = 6.8$ Hz, 2H), 7.27 (s, 1H), 6.92 (d, $J = 8.0$ Hz, 4H), 6.10 (s, 1H), 5.55 (s, 1H), 4.39 (t, $J = 4.4$ Hz, 2H), 1.81 (t, $J = 6.8$ Hz, 2H), 1.72 (t, $J = 7.2$ Hz, 2H), 1.53–1.46 (m, 4H). ^{13}C NMR (100 MHz): $\delta = 158.25, 157.69, 137.19, 136.45, 133.77, 132.91, 127.70, 127.59, 125.24, 123.36, 122.64, 114.82, 114.75, 70.30, 70.11, 69.61, 68.80, 67.83, 67.53, 64.63, 49.60, 36.18, 29.16, 28.52, 25.79, 25.75, 18.33$. IR (KBr): 3150, 3090, 2935, 2867, 1718, 1637, 1604, 1560, 1501, 1471, 1455, 1389, 1323, 1297, 1270, 1245, 1169, 1101, 1065, 987, 955, 930, 825 cm^{-1} . Elemental analysis calcd. (%) for $\text{C}_{32}\text{H}_{43}\text{BF}_4\text{N}_2\text{O}_6$: C, 60.19; H, 6.79; N, 4.39. Found: C, 58.72; H, 6.62; N, 4.31.

Synthesis of columnar liquid crystalline monomer 4. The synthesis of polymerizable ionic liquid **4** is outlined in scheme 4–3. The first step requires the protection of two phenol groups from the 3- and 5-positions of ethyl 3,4,5-trihydroxybenzoate. *Tert*-butyldimethylsilyl group as a bulky protecting group was employed for this purpose. The hydroxyl group of **16** was etherified with 1-dodecanol in toluene at room temperature by using diethylazodicarboxylate (DEAD) and triphenylphosphine (PPh₃) to give **17**. The silyl protecting group was cleaved with tetra-*n*-butylammonium fluoride (TBAF) to produce ethyl 3,5-dihydroxy-4-dodecyloxybenzoate **18**. The hydroxyl groups of **18** were etherified with 11-bromo-1-undecanol in *N,N*-dimethylformamide (DMF) at 70 °C by using K₂CO₃ as a base to yield **19**. The hydrolysis of **19** with an aqueous KOH in refluxing ethanol yielded the corresponding benzoic acid **20**. Compound **20** was esterified with acryloyl chloride using *N,N*-diethylaniline in dioxane at 60 °C. The intermediate benzoic acryloyl anhydride was hydrolyzed with pyridine and water at 100 °C to produce **21**. Finally, esterification of **21** and 1-(2-hydroxyethyl)-3-methylimidazolium tetrafluoroborate⁵⁰ was carried out in dichloromethane at room temperature by using dicyclohexylcarbodiimide (DCC) and *N,N*-dimethylaminopyridine (DMAP) to give diacrylate functionalized ionic liquid **4**.



Scheme 5–1. Synthesis of compound **4**. i) TBSCl, imidazole, DMF; ii) 1-Dodecanol, DEAD, PPh₃, toluene; iii) TBAF, CH₂Cl₂; iv) 11-Bromo-1-undecanol, K₂CO₃, DMF, 70 °C; v) NaOH/H₂O, EtOH; vi) HCl; vii) acryloyl chloride, *N,N*-diethylaniline, dioxane, 60 °C; viii) pyridine/H₂O, 100 °C; ix) 1-(2-Hydroxyethyl)-3-methylimidazolium⁺ tetrafluoroborate⁻, DCC, DMAP.

Synthesis of Ethyl 3,5-Bis[(*tert*-butyldimethylsilyloxy)-4-Hydroxybenzoate (**16**).

A solution of *tert*-butyldimethylsilyl chloride (TBSCl) (15.4 g, 102.2 mmol) in DMF (20 mL) was added dropwise to a solution of ethyl gallate (ethyl 3,4,5-trihydroxybenzoate) (10.1 g, 50.1 mmol) and imidazole (10.5 g, 154.4 mmol) in DMF (50 mL) at 0 °C. The reaction mixture was warmed up to room temperature and stirred for a further 12 h. Then water and ethyl acetate (EtOAc) were added, the organic layer was separated and washed with saturated NH₄Cl aqueous solution. The resulting organic phase was dried over anhydrous MgSO₄, filtered through a pad of Celite, and concentrated under vacuum. The residue was purified by flash-column chromatography on silica gel (eluent: hexane/chloroform = 2/1) to give **16** (14.9 g, 34.9 mmol) as a white solid. ¹H NMR (400 MHz, CDCl₃): δ = 7.22 (s, 2H), 5.65 (s, 1H),

4.31 (q, $J = 6.8$ Hz, 2H), 1.36 (t, $J = 7.0$ Hz, 3H), 1.00 (s, 18H), 0.24 (s, 12H); ^{13}C NMR (100 MHz, CDCl_3): $\delta = 166.29, 143.46, 142.77, 120.98, 114.68, 60.71, 25.67, 18.25, 14.29, -4.37$. IR (KBr): 3422, 2956, 2931, 2860, 1717, 1603, 1506, 1472, 1435, 1394, 1372, 1338, 1260, 1224, 1073, 1029, 841, 785 cm^{-1} .

Synthesis of Ethyl 3,5-Bis[(*tert*-butyldimethylsilyl)oxy]-4-dodecyloxybenzoate

(17). To a solution of PPh_3 (6.11 g, 23.3 mmol), 1-dodecanol (6.12 g, 32.9 mmol), and **16** (10.0 g, 23.5 mmol) in toluene (50 mL), DEAD (3.8 mL, 24.1 mmol) was added dropwise with stirring at room temperature. After stirring for 10 h at room temperature, the resulting mixture was poured into a mixture of water and EtOAc. The organic phase was separated and washed with a sat. aq. NaCl solution. The resulting organic phase was dried over anhydrous MgSO_4 , filtered through a pad of Celite, concentrated *in vacuo*. The residue was purified by silica gel column chromatography (eluent: hexane/chloroform = 2/1) to give **17** (13.2 g, 22.2 mmol) of as a viscous liquid. ^1H NMR (400 MHz, CDCl_3): $\delta = 7.19$ (s, 2H), 4.32 (q, $J = 6.8$ Hz, 2H), 3.94 (t, $J = 6.8$ Hz, 2H), 1.73 (t, $J = 7.2$ Hz, 3H), 1.26 (s, 20H), 1.00 (s, 18H), 0.88 (t, $J = 7.2$ Hz, 3H), 0.20 (s, 12H); ^{13}C NMR (100 MHz, CDCl_3): $\delta = 166.20, 149.59, 146.57, 124.84, 115.82, 72.92, 60.78, 31.91, 30.11, 29.64, 29.63, 29.57, 29.54, 29.35, 26.06, 25.87, 25.76, 22.68, 18.32, 14.29, 14.13, -4.48$. IR (KBr): 2956, 2929, 2857, 1721, 1577, 1490, 1472, 1428, 1391, 1369, 1346, 1254, 1215, 1094, 1032, 1006, 980, 831, 784 cm^{-1} .

Synthesis of Ethyl 3,5-dihydroxy-4-dodecyloxybenzoate (18). A 1.0 M solution of TBAF in tetrahydrofuran (50 mL, mmol) was added dropwise to a solution of compound **17** in dichloromethane (40 mL) at 0 °C. The mixture was stirred for 10 h at room temperature. The solution was poured into water and extracted with chloroform three times. The combined

organic phase was washed with brine, dried over anhydrous MgSO_4 , filtered through a pad of Celite, and concentrated with a rotary evaporator. The residue was purified by flash column chromatography on silica gel (eluent: chloroform) to afford **18** (8.12 g, 22.1 mmol) as a white solid. ^1H NMR (400 MHz, CDCl_3): δ = 7.30 (s, 2H), 6.29 (s, 2H), 4.34 (q, J = 6.8 Hz, 2H), 4.16 (t, J = 6.8 Hz, 2H), 1.77 (t, J = 7.6 Hz, 3H), 1.26 (s, 20H), 0.88 (t, J = 7.2 Hz, 3H); ^{13}C NMR (100 MHz, CDCl_3): δ = 166.85, 148.87, 137.75, 125.57, 109.64, 73.80, 61.33, 31.87, 30.10, 29.60, 29.59, 29.53, 29.49, 29.34, 29.31, 25.81, 22.65, 14.15, 14.08. IR (KBr): 3403, 2917, 2850, 1696, 1601, 1520, 1470, 1448, 1397, 1350, 1240, 1190, 1099, 1054, 1029, 877, 768 cm^{-1} .

Synthesis of Ethyl 3,5-bis(11-hydroxyundecyloxy)-4-dodecyloxybenzoate (19).

A DMF (50 mL) suspension of **18** (1.44 g, 3.92 mmol), 11-bromoundecan-1-ol (2.36 g, 9.41 mmol), and K_2CO_3 (1.38 g, 10.0 mmol) was vigorously stirred for 6 h at 70 $^\circ\text{C}$. After the resulting brown mixture was cooled to room temperature, the mixture was poured into a sat. NH_4Cl aqueous solution and extracted with EtOAc three times. The combined organic extracts were washed with brine. The resulting organic phase was dried over anhydrous MgSO_4 , filtered through a pad of Celite, and concentrated under reduced pressure. The residue was purified by flash column chromatography on silica gel (eluent: hexane/EtOAc = 5/1) to give **19** (2.60 g, 3.68 mmol) as a white solid. IR (KBr): 3464, 2918, 2850, 1704, 1590, 1505, 1470, 1431, 1392, 1340, 1264, 1229, 1130, 1059, 860, 766, 723 cm^{-1} .

Synthesis of 3,5-Bis(11-hydroxyundecyloxy)-4-dodecyloxybenzoic acid (20).

Compound **19** (2.60 g, 3.68 mmol) was dissolved in a mixture of ethanol/water (99:1 vol/vol, 100 mL) containing KOH (1.0 g, 18 mmol). After stirring for 3 h under a refluxed condition,

the solution was neutralized with a 1.0 M HCl aqueous solution and extracted with EtOAc twice. The combined organic phase was dried over anhydrous MgSO₄, filtered, and concentrated. The residue was recrystallized from ethanol to yield **20** (1.86 g, 2.74 mmol) as a white solid.

Synthesis of 3,5-Bis(11-acryloyloxyundecyloxy)-4-dodecyloxybenzoic acid (21).

To a solution of **20** (1.84 g, 2.71 mmol) and *N,N*-diethylaniline (1.21 g, 8.13 mmol) in 1,4-dioxane (100 mL), acryloyl chloride (0.74 g, 8.13 mmol) was added dropwise at 70 °C in a light resistant container and the reaction mixture was stirred for 3 h at 60 °C. After excess amount of acryloyl chloride was inactivated by the addition of methanol (10 mL), the mixture was concentrated by using rotary evaporator. The residue as a viscous liquid was dissolved in a mixture of pyridine (5 mL) and water (5 mL). The mixture was stirred for 1 h at 80 °C to cleave the benzoic acryloyl anhydride. Then, the mixture was acidified with HCl aq. solution (5 %), and extracted with EtOAc. The organic phase was washed with aq. NaHCO₃ solution (5%) and dried over anhydrous MgSO₄. The solvent was removed under reduced pressured. The crude product was purified by flash column chromatograph on silica gel (eluent: chloroform/methanol = 10/1) and then recrystallized from EtOAc to give **21** (1.52 g, 1.93 mmol) as a white solid. ¹H NMR (400 MHz, CDCl₃): δ = 7.32 (s, 2H), 6.40 (dd, *J* = 17, 1.4 Hz, 2H), 6.12 (dd, *J* = 17, 10 Hz, 2H), 5.82 (dd, *J* = 11, 1.4 Hz, 2H), 4.15 (t, *J* = 6.8 Hz, 4H), 4.04 (t, *J* = 6.8 Hz, 6H), 1.84–1.70 (m, 4H), 1.70–1.63 (m, 4H), 1.51–1.44 (m, 6H), 1.44–1.20 (m, 42H), 0.88 (t, *J* = 6.8, 3H); ¹³C NMR (100 MHz, CDCl₃): δ = 171.54, 166.37, 152.80, 143.02, 130.46, 128.59, 123.61, 108.45, 73.50, 69.11, 64.71, 38.17, 31.91, 30.28, 29.72, 29.70, 29.68, 29.66, 29.55, 29.52, 29.49, 29.36, 29.34, 29.25, 29.22, 28.57, 26.02, 26.00, 25.90, 22.67, 14.11. IR (KBr): 2920, 2851, 1726, 1683, 1620, 1586, 1505, 1472, 1432, 1410, 1386,

1335, 1295, 1275, 1228, 1200, 1122, 1058, 987, 966, 812, 723 cm^{-1} . Elemental analysis calcd. (%) for $\text{C}_{47}\text{H}_{78}\text{O}_9$: C, 71.72; H, 9.99. Found: C, 71.40; H, 10.15.

Synthesis of

3-{3,5-Bis(11-acryloyloxyundecyloxy)-4-dodecyloxybenzoyloxyethyl}-1-methylimidazolium tetrafluoroborate (4). To a mixture of **21** (1.00 g, 1.27 mmol), 1-(2-hydroxyethyl)-3-methylimidazolium tetrafluoroborate⁵⁰ (0.278 g, 1.30 mmol), and DMAP (1.6 mg, 0.012 mmol) in a mixture of dry CH_2Cl_2 /acetonitrile (1:1, vol/vol, 30 mL), DCC (0.262 g, 1.27 mmol) was added. The reaction mixture was stirred for 13 h at room temperature. After filtration of insoluble materials, the organic phase was concentrated in vacuum. The residue was purified by flash column chromatography on silica gel (eluent: $\text{CHCl}_3/\text{MeOH} = 10/1$) followed by GPC to give **4** (0.961 g, 9.78 mmol). ^1H NMR (400 MHz, CDCl_3): $\delta = 8.90$ (s, 1H), 7.35 (s, 1H), 7.26 (s, 1H), 7.19 (s, 2H), 6.39 (dd, $J = 17, 1.8$ Hz, 2H), 6.12 (dd, $J = 18, 10$ Hz, 2H), 5.82 (dd, $J = 10, 1.4$ Hz, 2H), 4.67–4.64 (m, 4H), 4.14 (t, $J = 7.0$ Hz, 4H), 4.03–3.98 (m, 6H), 3.95 (s, 3H), 1.84–1.70 (m, 4H), 1.70–1.63 (m, 4H), 1.51–1.44 (m, 6H), 1.44–1.20 (m, 42H), 0.88 (t, $J = 6.8, 3\text{H}$); ^{13}C NMR (100 MHz, CDCl_3): $\delta = 166.32, 165.77, 152.96, 142.94, 137.34, 130.43, 128.58, 123.27, 123.23, 122.66, 107.99, 73.52, 69.26, 64.66, 62.73, 49.00, 36.44, 31.89, 30.30, 29.71, 29.68, 29.65, 29.56, 29.53, 29.50, 29.49, 29.39, 29.35, 29.28, 29.23, 28.56, 26.08, 26.01, 25.89, 22.66, 14.09$. IR (KBr): 3155, 3091, 2921, 2851, 1726, 1699, 1635, 1587, 1505, 1469, 1432, 1410, 1387, 1338, 1298, 1271, 1200, 1130, 1063, 984, 855, 810, 762, 721 cm^{-1} . Elemental analysis calcd. (%) for $\text{C}_{53}\text{H}_{87}\text{BF}_4\text{N}_2\text{O}_9$: C, 64.75; H, 8.92; N, 2.85. Found: C, 64.15; H, 8.92; N, 2.85.

4.5. References

1. P. G. Bruce, C. A. Vincent, *J. Chem. Soc., Faraday Trans.* **1993**, *89*, 3187.
2. W. H. Meyer, *Adv. Mater.* **1998**, *10*, 439.
3. R. A. Colley, P. M. Budd, J. R. Owen, S. Balderson, *Polym. Int.* **2000**, *49*, 371.
4. T. Kato, *Science* **2002**, *295*, 2414.
5. K. Kishimoto, M. Yoshio, T. Mukai, M. Yoshizawa, H. Ohno, T. Kato, *J. Am. Chem. Soc.* **2003**, *125*, 3196.
6. V. Percec, J. A. Heck, D. Tomazos, G. Ungar, *J. Chem. Soc., Perkin Trans. 2* **1993**, 2381.
7. V. Percec, D. Tomazos, *J. Mater. Chem.* **1993**, *3*, 633.
8. H. V. St. A. Hubbard, S. A. Sills, G. R. Davies, J. E. McIntyre, I. M. Ward, *Electrochim. Acta* **1998**, *43*, 1239.
9. Imrie, C. T.; Ingram, M. D.; McHattie, G. S. *Adv. Mater.* **1999**, *11*, 832.
10. F. B. Dias, S. V. Batty, G. Ungar, J. P. Voss, P. V. Wright, *J. Chem. Soc., Faraday Trans.* **1996**, *92*, 2599.
11. C. F. van Nostrum, R. J. M. Nolte, *Chem. Commun.* **1996**, 2385.
12. U. Beginn, G. Zipp, A. Mourran, P. Walther, M. Möller, *Adv. Mater.* **2000**, *12*, 513.
13. U. Lauter, W. H. Meyer, G. Wegner, *Macromolecules* **1997**, *30*, 2092.
14. T. Ohtake, K. Ito, N. Nishina, H. Kihara, H. Ohno, T. Kato, *Polym. J.* **1999**, *31*, 1155.
15. T. Ohtake, M. Ogasawara, K. Ito-Akita, N. Nishina, S. Ujiie, H. Ohno, T. Kato, *Chem. Mater.* **2000**, *12*, 782.
16. T. Ohtake, Y. Takamitsu, K. Ito-Akita, K. Kanie, M. Yoshizawa, T. Mukai, H. Ohno, T. Kato, *Macromolecules* **2000**, *33*, 8109.
17. T. Ohtake, K. Kanie, M. Yoshizawa, T. Mukai, K. Ito-Akita, H. Ohno, T. Kato, *Mol.*

- Cryst. Liq. Cryst.* **2001**, *364*, 589.
18. K. Hoshino, K. Kanie, T. Ohtake, T. Mukai, M. Yoshizawa, S. Ujiie, H. Ohno, T. Kato, *Macromol. Chem. Phys.* **2002**, *203*, 1547.
 19. J. S. Wilkes, M. J. Zaworotko, *J. Chem. Soc., Chem. Commun.* **1992**, 965.
 20. P. Bonhôte, A.-P. Dias, N. Papageorgiou, K. Kalyanasundaram, M. Grätzel, *Inorg. Chem.* **1996**, *35*, 1168.
 21. D. R. MacFarlane, P. Meakin, J. Sun, N. Amini, M. Forsyth, *J. Phys. Chem. B* **1999**, *103*, 4164.
 22. H. Ohno, *Electrochim. Acta* **2001**, *46*, 1407.
 23. M. Yoshizawa, H. Ohno, *Electrochim. Acta* **2001**, *46*, 1723.
 24. M. Yoshizawa, M. Hirao, K. Ito-Akita, H. Ohno, *J. Mater. Chem.* **2001**, *11*, 1057.
 25. A. Noda, M. Watanabe, *Electrochim. Acta* **2000**, *45*, 1265.
 26. S. Ujiie, K. Iimura, *Polym. J.* **1993**, *25*, 347.
 27. V. Hessel, H. Ringsdorf, *Makromol. Chem. Rapid Commun.* **1993**, *14*, 707.
 28. C. Chovino, Y. Frere, D. Guillon, P. Gramain, *J. Polym. Sci. PartA: Polym. Chem.* **1997**, *35*, 2569.
 29. S. Takada, N. Suzuki, T. Mihara, N. Koide, *Polym. Prepr. Jpn.* **2002**, *51*, 737.
 30. D. J. Broer, H. Finkelmann, K. Kondo, *Makromol. Chem.* **1988**, *189*, 185.
 31. R. A. M. Hikmet, *J. Mater. Chem.* **1999**, *9*, 1921.
 32. A. Mueller, D. F. O'Brien, *Chem. Rev.* **2002**, *102*, 727.
 33. D. F. O'Brien, B. Armitage, A. Benedicto, D. E. Bennett, H. G. Lamparski, Y.-S. Lee, W. Srisiri, T. M. Sisson, *Acc. Chem. Res.*, **1998**, *31*, 861.
 34. H. Kuroda, H. Goto, K. Akagi, A. Kawaguchi, *Macromolecules* **2002**, *35*, 1307.
 35. T. Kato, Y. Kubota, T. Uryu, *Polym. Bull.* **1997**, *38*, 551.

-
36. K.-S. Kim, T. Kato, T. Uryu, *J. Polym. Sci. PartA: Polym. Chem.* **1999**, *37*, 3877.
37. S. I. Stupp, S. Son, H. C. Lin, L. S. Li, *Science* **1993**, *259*, 59.
38. (a) V. Percec, J. Heck, D. Tomazos, F. Falkenberg, H. Blackwell, G. Unger, *J. Chem. Soc., Perkin Trans. 1*, **1993**, 2799; (b) V. Percec, D. Tomazos, J. Heck, H. Blackwell, G. Ungar, *J. Chem. Soc., Perkin Trans. 2*, **1994**, 31; (c) V. Percec, J. Heck, D. Tomazos, G. Ungar, *J. Chem. Soc., Perkin Trans. 2*, **1993**, 2381; (d) Y. K. Kwon, S. N. Chvalun, J. Blackwell, V. Percec, J. A. Heck, *Macromolecules*, **1995**, *28*, 1552; (e) V. Percec, D. Schlueter, Y. K. Kwon, J. Blackwell, M. Möller, P. J. Slangen, *Macromolecules*, **1995**, *28*, 8807; (f) V. Percec, D. Schlueter, G. Ungar, S. Z. D. Cheng, A. Zhang, *Macromolecules*, **1998**, *31*, 1745; (g) V. Percec, T. K. Bera, *Tetrahedron*, **2002**, *58*, 4031.
39. D. L. Gin, W. Gu, B. A. Pindzola, W.-J. Zhou, *Acc. Chem. Res.*, **2001**, *34*, 973.
40. W. Srisiri, T. M. Sisson, D. F. O'Brien, K. M. McGrath, Y. Han, S. M. Gruner, *J. Am. Chem. Soc.*, **1997**, *119*, 4866.
41. H. Ringsdorf, B. Schlarb, J. Venzmer, *Angew. Chem. Int. Ed. Engl.*, **1988**, *27*, 113.
42. H.-K. Lee, Y. H. Ko, Y. J. Chang, N.-K. Oh, W.-C. Zin, K. Kim, *Angew. Chem. Int. Ed.*, **2001**, *40*, 2669.
43. Y. Ishida, S. Amano, K. Saigok, *Chem. Commun.*, **2003**, 2338.
44. (a) U. Beginn, G. Zipp, M. Möller, *Adv. Mater.*, **2000**, *12*, 510; (b) U. Beginn, G. Zipp, A. Mourran, P. Walther, M. Möller, *Adv. Mater.*, **2000**, *12*, 513; (c) U. Beginn, G. Zipp, M. Möller, *Chem. Eur. J.*, **2000**, *6*, 2016.
45. (a) S. A. Miller, J. H. Ding, D. L. Gin, *Curr. Opin. Colloid Interface Sci.*, **1999**, *4*, 338; (b) B. A. Pindzola, B. P. Hoag, D. L. Gin, *J. Am. Chem. Soc.*, **2001**, *123*, 4617; (c) R. C. Smith, W. M. Fischer, D. L. Gin, *J. Am. Chem. Soc.*, **1997**, *119*, 4092; (d) B. P. Hoag, D.

- L. Gin, *Macromolecules*, **2000**, *33*, 8549; (e) W. Zhou, W. Gu, Y. Xu, C. S. Pecinovsky, D. L. Gin, *Langmuir*, **2003**, *19*, 6346.
46. (a) D. L. Gin, W. Gu, *Adv. Mater.*, **2001**, *13*, 1407; (b) J. H. Ding, D. L. Gin, *Chem. Mater.*, **2000**, *12*, 22; (c) W. Gu, W.-J. Zhou, D. L. Gin, *Chem. Mater.*, **2001**, *13*, 1949; (d) D. L. Gin, H. Deng, W. M. Fischer, D. H. Gray, E. Juang, E. Kim, R. C. Smith, *Mol. Cryst. Liq. Cryst.*, **1999**, *332*, 423.
47. J. F. van der Pol, E. Neeleman, J. C. van Miltenburg, J. W. Zwikker, R. J. M. Nolte, W. Drenth, *Macromolecules*, **1990**, *23*, 155.
48. K. Borisch, S. Diele, P. Göring, H. Kresse, C. Tschierske, *J. Mater. Chem.*, **1998**, *8*, 529.
49. O. Mitsunobu, M. Yamada, T. Mukaiyama, *Bull. Chem. Soc. Jpn.* **1967**, *40*, 935.
50. W. Miao, T. H. Chan, *Org. Lett.*, **2003**, *5*, 5003.

Chapter 5

Conclusions

This thesis describes the development of anisotropic ion-transporting materials by self-organization of ionic liquids. The author prepared novel liquid crystalline materials based on ionic liquids. One- and two-dimensional ion transportation in the liquid crystalline nanostructures was achieved for the first time by controlling the self-assembled structures ranging from molecular to macroscopic scales.

In Chapter 1, an overview of ionic liquids and liquid crystals is described. Previous studies on development of anisotropic organic ion conductors are introduced. The objectives of this thesis are also given.

In Chapter 2, liquid crystalline composite materials consisting of ionic liquids and designed liquid crystals were prepared. Rod-like and fan-like mesogenic molecules having hydroxyl groups were synthesized as structure-inducing molecules that can interact with conventional isotropic ionic liquids. Supramolecular self-assemblies which have nanophase-segregated layered and columnar structures are spontaneously formed by simply mixing ionic liquids with rod-like and fan-like mesogenic molecules, respectively. Such assemblies exhibit thermally stable liquid crystalline phases compared to that of mesogenic molecules alone. The author supposed that the mesophase stabilization was due to the hydrogen bonding between ionic liquids and hydroxyl groups. The formation of hydrogen bonding in the assembled materials is revealed by the IR and NMR measurements. For smectic liquid crystalline assemblies, homeotropic alignment on the surface of glassy and ITO substrates was spontaneously achieved due to the interaction between the surface of substrates and ionic liquids or hydroxyl groups. On the other hand, macroscopically uniaxial orientation of columnar assemblies was achieved by shearing the materials which is sandwiched between two glassy substrates. Anisotropic ionic conductivities were successfully measured for these oriented materials for the first time.

In Chapter 3, new ionic molecules programmed to form columnar liquid crystalline phases were synthesized as a new family of single ion conductors. In the self-organized columns, only anion can move long distance along the direction of the column axis. Liquid crystalline properties and ionic conductivities of the ion-active materials were examined. The choice of appropriate anion species and the length of alkyl chains led to the development of ionic materials showing liquid crystalline phases at wide temperature ranges and high anisotropy of ionic conductivities.

In Chapter 4, self-standing polymer films with layered and columnar nanostructures were prepared by in situ photopolymerization of polymerizable ionic liquid crystalline molecules. The method to prepared ion-conductive polymer films with well-defined nanostructures is descried. To improve ion-conductive properties of the films, ion-conductive monomer is chemically modified.

List of Publications

Original Papers

- (1) “Layered Ionic Liquids: Anisotropic Ion Conduction in New Self-Organized Liquid-Crystalline Materials”
Masafumi Yoshio, Tomohiro Mukai, Kisyoshi Kanie, Masahiro Yoshizawa, Hiroyuki Ohno, and Takashi Kato
Adv. Mater., **14**, 351 (2002).

- (2) “Liquid-Crystalline Assemblies Containing Ionic Liquids: An Approach to Anisotropic Ionic Materials”
Masafumi Yoshio, Tomohiro Mukai, Kiyoshi Kanie, Masahiro Yoshizawa, Hiroyuki Ohno, and Takashi Kato
Chem. Lett., **2002**, 320.

- (3) “Nanostructured Ion-Conductive Films: Layered Assembly of a Side-Chain Liquid-Crystalline Polymer with an Imidazolium Ionic Moiety”
Koji Hoshino, Masafumi Yoshio, Kenji Kishimoto, Tomohiro Mukai, Hiroyuki Ohno, and Takashi Kato
J. Polym. Sci., Part A, Polym. Chem., **41**, 3486 (2003).

- (4) “One-Dimensional Ion Transport in Self-Organized Columnar Ionic Liquids”
Masafumi Yoshio, Tomohiro Mukai, Hiroyuki Ohno, and Takashi Kato
J. Am. Chem. Soc., **126**, 994 (2004).

- (5) “Self-Assembly of an Ionic Liquid and a Hydroxyl-Terminated Liquid Crystal: Anisotropic Ion Conduction in Layered Nanostructures”
Masafumi Yoshio, Tomohiro Mukai, Masahiro Yoshizawa, Hiroyuki Ohno, and Takashi Kato
Mol. Cryst., Liq. Cryst., **431**, 2235 (2004).

Books

- (1) Masafumi Yoshio and Takashi Kato, “Liquid-Crystalline Ionic Liquids” in “Ionic Liquids: The Front and Future of Material Developments” H. Ohno Ed., CMC, Tokyo, 2003, Chapter 5. 6, p.161. (in Japanese)
- (2) Takashi Kato and Masafumi Yoshio, “Liquid Crystalline Ionic Liquids” in “Electrochemical Aspects of Ionic Liquids” H. Ohno Ed., John Wiley & Sons, Inc., in press.

References

- (1) “Nanostructured Anisotropic Ion-Conductive Films”
Kenji Kishimoto, Masafumi Yoshio, Tomohiro Mukai, Masahiro Yoshizawa, Hiroyuki Ohno, and Takashi Kato
J. Am. Chem. Soc., **125**, 3196 (2003).
- (2) “Effect of Methyl Groups onto Imidazolium Cation Ring on Liquid Crystallinity and Ionic Conductivity of Amphiphilic Ionic Liquids”
Tomohiro Mukai, Masafumi Yoshio, Takashi Kato, and Hiroyuki Ohno
Chem. Lett., **2004**, 1630.

List of Publications

- (3) “Anisotropic Ion Conduction in a Unique Smectic Phase of Self-Assembled Amphiphilic Ionic Liquids”

Tomohiro Mukai, Masafumi Yoshio, Takashi Kato, and Hiroyuki Ohno

Chem. Commun., in press.

- (4) “Self-assembled N-Alkylimidazolium Perfluorooctanesulfonate”

Tomohiro Mukai, Masafumi Yoshio, Takashi Kato, and Hiroyuki Ohno

Chem. Lett., in press.

- (5) “Enthalpy Relaxation Behavior of Liquid-Crystalline Glasses of an Esterified Cholesterol Derivative and its Complex Salts with Aliphatic Amines”

Masafumi Yoshio, Yoshiharu Miyashita, and Yoshiyuki Nishio

Mol. Cryst. Liq. Cryst., **357**, 27 (2001).

Patent

- (1) Takashi Kato, Kiyoshi Kanie, Masafumi Yoshio, Hiroyuki Ohno, and Masahiro Yoshizawa, Jpn. Kokai Tokkyo Koho 358, 821 (2002).

Acknowledgements

The research works presented in this thesis were carried out under the supervision of Professor Takashi Kato at the University of Tokyo from 2000 to 2005.

First of all, the author would like to thank Professor Takashi Kato at the University of Tokyo for his continual guidance and stimulating supervision throughout the present work. I have learned numerous things from him with respect to supramolecular chemistry and beyond. I am very grateful for accepting me as a research associate of his laboratory.

The author is deeply grateful to Professor Kazuhiko Saigo, Professor Kyoko Nozaki, Associate Professor Hiroyuki Asanuma, and Associate Professor Kazuaki Kudo who gave him valuable and helpful advices for improving and summarizing this work.

The author appreciates Professor Hiroyuki Ohno at Tokyo University of Agriculture and Technology for helpful discussion and the measurements of ionic conductivities. The author also acknowledges Dr. Masahiro Yoshizawa, Tomohiro Mukai for the measurements of ionic conductivities and fruitful discussions.

The author expresses his gratitude to Dr. Kiyoshi Kanie, Dr. Masaya Moriyama, Dr. Emmanuel Marfo-Owusu, Mr. Kenji Kishimoto, Mr. Koji Hoshino, Mr. Go Yamashita, Mr. Yusuke Tochigi, Mr. Tomoki Yokota, Mr. Takayoshi Kagata, Mr. Harutoki Shimura, Ms. Yuko Kamikawa, Ms. Yuko Watanabe, Mr. Tatsuya Koga, and Ms. Sanami Yazaki for collaborations in Kato Laboratory. They made author's research life significant and delightful through experiments and discussion. Especially, I wish to thank Mr. Yusuke Tochigi for his mental health care. My life would be difficult without his help. The author is also grateful to his colleagues Dr. Norihiro Mizoshita, Dr. Kazuhiro Yabuuchi, Dr. Ayae Sugawara, Mr. Masayuki Nishii, Mr. Toru Matsuoka, and every member in Kato Laboratory. They

Acknowledgements

encouraged and helped the author when the author has been appointed as a research associate at the University of Tokyo in June 2002. I am very grateful to Dr. Etienne Baranoff for correcting this thesis.

This research was partially supported by Grant-in-aid for Scientific Research on Priority Areas, Scientific Research B, Encouragement of Young Scientists B, and The 21st Century COE Program from the Ministry of Education, Culture, Sports, Science, and Technology is gratefully acknowledged.

Finally, the author sincerely acknowledges his parents, Yasumasa and Kei Yoshio, and his brother Hideaki Yoshio for their constant support and encouragement.

February, 2005



Masafumi YOSHIO